AD-A257 698

NAVAL POSTGRADUATE SCHOOL
Monterey, California

DTIC
ELECTE
DEC 0 3 1992
S B D

THESIS

SIMULATION OF THE UNDERWATER NUCLEAR EXPLOSION AND ITS EFFECTS

by

William Earl Miller II

JUNE 1992

Thesis Advisor: Young W. Kwon

Approved for public release; distribution is unlimited.

92-30725

Unclassified
SECURITY CLASSIFICATION OF THIS PAGE

REPORT DOCUMENTATION PAGE

Form Approved
OMB No 0704-0188

1a REPORT SECURITY CLASSIFICATION Unclassified	1b RESTRICTIVE MARKINGS
2a SECURITY CLASSIFICATION AUTHORITY	3 DISTRIBUTION / AVAILABILITY OF REPORT Approved for public release: Distribution is Unlimited
2b DECLASSIFICATION / DOWNGRADING SCHEDULE	
4 PERFORMING ORGANIZATION REPORT NUMBER(S)	5 MONITORING ORGANIZATION REPORT NUMBER(S)
6a NAME OF PERFORMING ORGANIZATION Naval Postgraduate School 6b OFFICE SYMBOL (If applicable) ME	7a NAME OF MONITORING ORGANIZATION Naval Postgraduate School
6c. ADDRESS (City, State, and ZIP Code) Monterey, CA 93943-5000	7b. ADDRESS (City, State, and ZIP Code) Monterey, CA 93943-5000
8a. NAME OF FUNDING / SPONSORING ORGANIZATION 8b. OFFICE SYMBOL (If applicable)	9. PROCUREMENT INSTRUMENT IDENTIFICATION NUMBER
8c. ADDRESS (City, State, and ZIP Code)	10 SOURCE OF FUNDING NUMBERS PROGRAM ELEMENT NO. / PROJECT NO. / TASK NO. / WORK UNIT ACCESSION NO.

11. TITLE (Include Security Classification)

SIMULATION OF THE UNDERWATER NUCLEAR EXPLOSION AND ITS EFFECTS (U)

12. PERSONAL AUTHOR(S)
WILLIAM E. MILLER II

13a TYPE OF REPORT	13b TIME COVERED	14. DATE OF REPORT (Year, Month, Day)	15 PAGE COUNT
Master's Thesis	FROM _____ TO _____	JUNE 1992	84

16 SUPPLEMENTARY NOTATION
The views expressed are those of the author and do not reflect the official policy or position of the Department of Defense or the U. S. Government.

17 COSATI CODES			18. SUBJECT TERMS (Continue on reverse if necessary and identify by block number)
FIELD	GROUP	SUB-GROUP	nuclear underwater shock

19 ABSTRACT (Continue on reverse if necessary and identify by block number)

This research was conducted to enhance understanding of the use of high explosives to simulate the effects of a nuclear underwater explosion. A review of the known characteristics of the nuclear, spherical conventional, and tapered conventional underwater pressure-time histories illustrates the selection of the tapered charge to simulate the underwater nuclear explosion. Three areas of study were then pursued. The first compared the structural response resulting from attack by conventional and nuclear type pressure profiles, verifying the need to match duration as well as peak pressure when simulating the underwater nuclear explosion. The second employed finite element analysis to study the three dimensional shock generated by a tapered charge. Third, a computer program was written to couple an optimizer with an existing tapered charge pressure-profile generating code to improve the tapered charge design process.

20 DISTRIBUTION / AVAILABILITY OF ABSTRACT ☒ UNCLASSIFIED/UNLIMITED ☐ SAME AS RPT ☐ DTIC USERS	21 ABSTRACT SECURITY CLASSIFICATION Unclassified
22a NAME OF RESPONSIBLE INDIVIDUAL Young W. Kwon	22b TELEPHONE (Include Area Code) (408) 646-3385 22c OFFICE SYMBOL ME/kw

DD Form 1473, JUN 86 Previous editions are obsolete

SECURITY CLASSIFICATION OF THIS PAGE
Unclassified

S/N 0102-LF-014-6603

Approved for public release: Distribution is unlimited

Simulation of the Underwater Nuclear Explosion and Its Effects

by

William Earl Miller II
Lieutenant, United States Navy
B. S., University of Missouri, Columbia, 1973

Submitted in partial fulfillment of the
requirements for the degree of

MASTER OF SCIENCE
IN MECHANICAL ENGINEERING

and

MECHANICAL ENGINEER

from the

NAVAL POSTGRADUATE SCHOOL

JUNE 1992

Author: William Earl Miller II

Approved by : Young Wook Kwon
Young W. Kwon, Thesis Advisor

Young S. Shin
Young S. Shin, Second Reader

Anthony J. Healey
Anthony J. Healey, Chairman
Department of Mechanical Engineering

Richard S. Elster
Richard S. Elster, Dean of Instruction

ABSTRACT

This research was conducted to enhance understanding of the use of high explosives to simulate the effects of a nuclear underwater explosion. A review of the known characteristics of the nuclear, spherical conventional, and tapered conventional underwater pressure-time histories illustrates the selection of the tapered charge to simulate the underwater nuclear explosion. Three areas of study were then pursued. The first compared the structural response resulting from attack by conventional and nuclear type pressure profiles, verifying the need to match duration as well as peak pressure when simulating the underwater nuclear explosion. The second employed finite element analysis to study the three dimensional shock generated by a tapered charge. Third, a computer program was written to couple an optimizer with an existing tapered charge pressure-profile generating code to improve the tapered charge design process.

Accession For
NTIS GRA&I ☑
DTIC TAB ☐
Unannounced ☐
Justification
By
Distribution/
Availability Codes
Dist | Avail and/or Special
A-1

TABLE OF CONTENTS

I. INTRODUCTION 1

II. CHARACTERISTICS AND MODELING OF THE UNDERWATER NUCLEAR EXPLOSION 4
- A. THE UNDERWATER NUCLEAR SHOCK PROFILE 4
- B. SPHERICAL CONVENTIONAL CHARGE PROFILE 9
- C. HOPKINSON SCALING 11
- D. TAPED CHARGE PRESSURE PROFILE 14

III. EFFECT OF PRESSURE DURATION ON STRUCTURAL RESPONSE 18
- A. ATTACK CURVES 18
- B. NUMERICAL MODEL 19
- C. RESULTS 22

IV. THE TAPERED CHARGE SHOCK FRONT 25
- A. FEA MODEL 25
- B. RESULTS 29
  - 1. Early Time Shape of the Shock Front 31
  - 2. Directionality of Peak Pressure 36

V. TAPERED CHARGE DESIGN OPTIMIZATION 44
- A. SIMPLE PRESSURE-TIME HISTORY ALGORITHM 44
- B. OPTIMIZATION PROBLEM 46
- C. OPTIMIZATION PROGRAM 47
  - 1. Required Program Input 48
  - 2. Program Output 50
- D. OPTIMIZATION RESULTS 52

VI. CONCLUSIONS AND RECOMMENDATIONS 54

APPENDIX A: TAPERED CHARGE FEM INPUT FILE 55
APPENDIX B: GRUNEISEN GAMMA APPROXIMATION 61
APPENDIX C: FORTRAN PROGRAM 63
I. PROGRAM DTAPOPT 63
II. SUBROUTINE DCOMPAR 70
III. SUBROUTINE DPTGEN 71
IV. SUBROUTINE DTAPWT 72

LIST OF REFERENCES 74
INITIAL DISTRIBUTION LIST 76

ACKNOWLEDGEMENTS

I express my sincere thanks and appreciation to Dr. Young W. Kwon and Dr. Young S. Shin for their continued support, guidance, and encouragement throughout this research. To Fred Costanzo of the Underwater Explosions Research Division of the David Taylor Research Center goes my deep appreciation for indoctrination into tapered charge design. I gratefully acknowledge the continued support of the underwater shock research at the Naval Postgraduate School by Dr. Thomas Tsai, Dr. Kent Goering, Doug Bruder, and the Defense Nuclear Agency. To LT Jim Chisum and LCDR Pad Fox, with whom I spent many hours and learned much, I extend my warmest personal thanks. For technical support and timely information I thank Dr. John Deruntz; Dr. John Hallquist, Dr. Doug Stillman, and staff; Dan Steinberg; and Dr. Mohsen Sanai.

Many others not mentioned by name, including fellow underwater shock researchers, provided welcome assistance. To you, please forgive the omission. I thank all of you.

I dedicate this work to my wife Maria and two daughters, Jolene and Steffany, for their support and understanding over the duration of this project.

I. INTRODUCTION

This thesis addresses efforts to improve simulation, using conventional high explosives and scale models, of the underwater shock environment and structural effects resulting from the underwater nuclear explosion. Simulation using scale models and small conventional charges provides valuable information without the requirement for nuclear testing, with minimal environmental impact, and at low cost. Better understanding of the physics involved impacts ship and weapons designs.

In the current atmosphere of reduced military spending in order to reap the benefits of the "Peace Dividend" resulting from the end of the cold war, the threat to U. S. Navy ships and submarines from underwater nuclear explosion would appear to be greatly reduced. However, two factors ensure the continued existence of the threat from underwater nuclear explosion:

1. The presence of the former Soviet Union's vast arsenal of nuclear weapons combines with economic instability to increase the likelihood of more nations gaining access to the material necessary to construct nuclear weapons.

2. The ceaseless march of technology worldwide dictates future growth in the number of nations attaining the particular technology necessary to build and detonate nuclear weapons.

The growing community of nuclear weapons capable nations may not posses the same restraint from the use of nuclear weapons displayed since 1945.

Given the existence of a threat from underwater nuclear explosion, the significance of this threat can be determined only if the effects are well understood. This same understanding is essential to incorporation of shock hardening in ship and submarine designs to improve survivability.

With the overall objective of improving ship and submarine survivability through better understanding of the phenomena associated with underwater explosions, the Naval Postgraduate School conducts ongoing research into underwater explosions and effects. This thesis is the result of a part of that continuing research, the first at the school related specifically to the nuclear underwater explosion.

The known characteristics of the nuclear underwater explosion, together with a discussion of modeling techniques is found in Chapter II.

Chapter III presents a comparison of the structural response of a simple cylinder subjected to side-on attack by conventional spherical charge and nuclear type pressure profiles. The doubly asymptotic boundary assumption combined with an explicit finite element method was used to perform the analysis. Results verify the need to match peak pressure and duration of the nuclear pressure-time history when designing test charges to simulate the underwater nuclear explosion.

The tapered charge, due to inherent long pressure duration, commonly generates the simulated nuclear pressure field used in model testing. Chapter IV explores the three dimensional aspects of the shock front generated by a conventional underwater tapered charge explosion. The results of analysis performed using an explicit finite element method are presented with the intent of supplementing existing knowledge of the tapered charge pressure profile which to date consists mostly of on-axis data. The results show the evolving shape of the shock front at early times and provide information on the relationship between the peak pressures measured on and off the charge axis.

As outlined in Chapter V, a computer code was written to optimize the design process for a conventional tapered high explosive charge. Starting with a desired pressure-time history and initial estimates for charge geometry and standoff distance, this program utilizes public domain optimization software to return improved design values. Although tested with a subroutine based upon an existing routine for calculating the pressure-time history of a tapered charge, this program may be coupled with other existing or future routines for calculating the tapered charge pressure-time history.

Conclusions and recommendations for further research in this area may be found in Chapter VI.

II. CHARACTERISTICS AND MODELING OF THE UNDERWATER NUCLEAR EXPLOSION

Before attempting to simulate the underwater nuclear explosion using conventional high explosive charges for scale model testing, a degree of familiarity with the shock generated by nuclear and spherical high explosive charges is warranted. This chapter, therefore, outlines the use of empirical relationships to determine the pressure-time histories generated by the two types of charges. The tremendous weight and standoff distance required for a conventional spherical charge to create a pressure profile similar to that of a nuclear charge points directly to the need for scaling.

Following a brief description of the principles used to construct scale models for underwater shock testing, these principles are applied to nuclear and conventional spherical charges. The resultant large size and standoff, even after scaling, of the conventional spherical charge, leads to the selection of the tapered charge, made of conventional high explosives, to simulate the underwater shock generated by the underwater nuclear explosion.

A. THE UNDERWATER NUCLEAR SHOCK PROFILE

The energy content, or "yield", of a nuclear explosion is commonly measured in tons of TNT equivalent, the amount of explosive energy contained in 2,000 pounds of the conventional high explosive TNT. A one kiloton (kT) device contains the energy equivalent of 1,000 tons of TNT, one megaton (MT) that of 1,000,000 tons. Although the majority of the energy released in an underwater nuclear explosion contributes to the generation of

the underwater shock wave, the extremely high temperatures (tens of millions of degrees) reached in a nuclear explosion contribute to a significant amount of energy release in the form of thermal radiation. Chemical explosions, by contrast, occur at much lower temperatures (thousands of degrees), resulting in a higher percentage of the total energy released as kinetic energy to generate the underwater shock. (Glasstone and Dolan, 1977, pp. 1-3, 6, 11)

To date, the United States has conducted five announced underwater nuclear explosions, from 1946 to 1962 (Bolt, 1976, pp. 251-274). Glasstone and Dolan (1977, pp. 268-272) provide three empirical charts to calculate the pressure-time history of an underwater nuclear explosion given the yield of the device and the standoff distance R from the explosion. From the curves of the first two charts, the maximum pressure P_{max} (psi) and the time constant θ (ms) are determined. The time constant equals, as in exponential decay, the time between the arrival of the shock when $P = P_{max}$ and the time at which $P = P_{max}/e \approx 0.37P_{max}$. The pressure actually decays at a somewhat slower than exponential rate after one time constant, necessitating the third chart which plots the non-dimensional values $P(t)/P_{max}$ vs t/θ to provide an idealized pressure-time history for an underwater nuclear explosion with no bottom or surface reflection effects. Based upon these curves, Figure 1 shows the pressure time history of a 40 kT nuclear explosion at a standoff of 1,000 yds. Figure 2 illustrates standoff. Two prominent features of the underwater nuclear explosion stand out in Figure 1: the high pressure at a significant distance from the explosion, and the long decay time. P_{max}

increases with yield, decreases with standoff; the duration of the shock wave increases with yield and standoff (Glasstone and Dolan, 1977, p. 269).

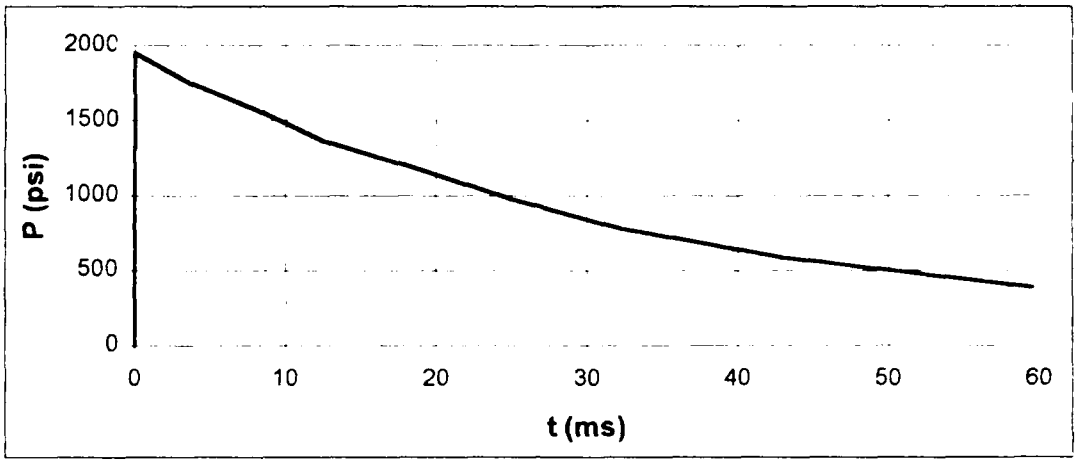

Figure 1. *Pressure profile of a 40 kT nuclear charge, R = 1000 yds.*

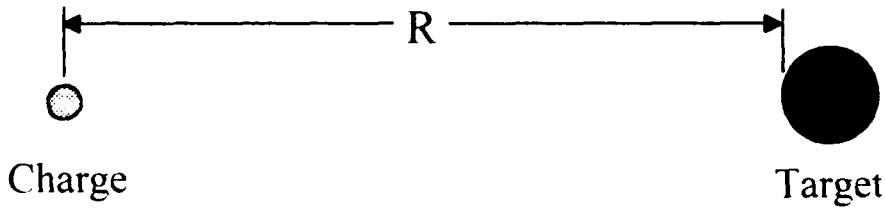

Figure 2. *Measurement of standoff distance R.*

In water of sufficient depth where bottom reflections are negligible or occur at a much later time, the steady pressure decay ends abruptly by the phenomenon of surface cutoff (Shin and Geers, 1991, §3.3; or Glasstone and Dolan, 1977, pp. 244-246). Figure 3 shows two paths followed by a shock wave emanating from an underwater explosion. The direct, compression wave strikes the target first with a sudden rise in pressure followed by the steady pressure decay described above. The other path shows a compression

wave striking the air-water interface and being reflected as a tension, or rarefaction wave.

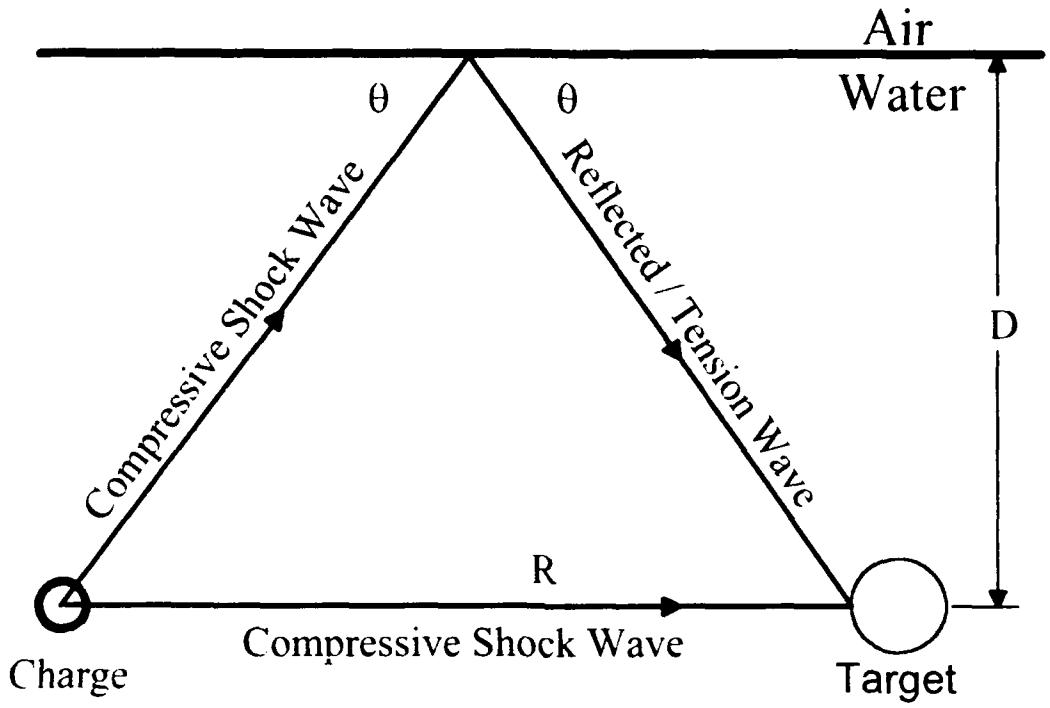

Figure 3. *Paths followed by the direct and rarefaction waves.*

Approximating shock speed by the speed of sound in water C_s gives the cutoff time t_{co} as the difference in distance traveled by the direct and rarefaction waves divided by C_s:

$$t_{co} = \frac{2\sqrt{\left(\frac{R}{2}\right)^2 + D^2} - R}{C_s}$$

The arrival of the rarefaction wave at time t_{co} after the arrival of the direct shock wave causes a sudden pressure drop as the remaining pressure from the compression wave is essentially canceled. Hence, if the 40 kT

nuclear charge discussed earlier is detonated at a 285 ft depth in deep water, a target at 1,000 yards and the same depth will experience t_c = 10.7 ms using the expression on the previous page with C_s = 5 ft/ms. The resultant pressure profile with pressure cutoff is shown in Figure 4.

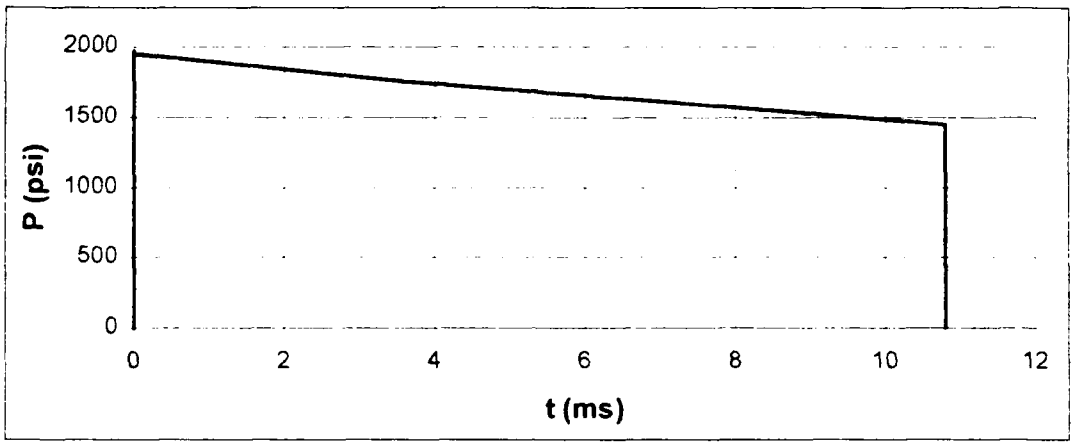

Figure 4. *Pressure profile of a 40 kT nuclear charge with surface cutoff. R=1,000 yds, D=285 ft.*

For an actual underwater nuclear explosion, the smooth curve of Figure 4 would be further modified by refraction of the shock wave due to salinity, currents, and temperature variation in the water media. Whereas Figure 4 depicts an instantaneous pressure rise upon arrival of the compression wave at time 0, a finite rise time would be expected. Additionally, the abrupt surface cutoff shown assumes the rarefaction wave and the compression wave travel at the same speed of sound in water. In actuality, the rarefaction wave travelling in shocked media partially overtakes the compression wave rendering a less steep pressure drop at t_c. For explosions occurring in shallow water, bottom reflections and retransmissions further alter the shock profile. Additional shocks may occur at later times due to the

bubble pulse resulting from explosions at depths such that the gases of the explosion expand and collapse before venting at the surface. More than three bubble pulses are unlikely due to steam condensation. (Glasstone and Dolan, 1977, pp. 56, 245, 246, 269)

Having established the general characteristics of the pressure-time history of the underwater nuclear explosion, the next section uses empirical formulas to determine the feasibility of emulating this profile using conventional high explosives of spherical shape.

B. SPHERICAL CONVENTIONAL CHARGE PROFILE

As in the case of the nuclear charge, the conventional charge of spherical or near spherical shape gives rise to a sudden pressure increase followed by exponential pressure decay for one time constant θ and somewhat slower decay thereafter. Using exponential pressure decay for an approximation, empirical studies provide the following useful relationships for determining the pressure-time history developed by a conventional high explosive of spherical or near spherical shape when detonated underwater (Shin and Geers, 1991, §3.2):

$$P(t) = P_{max} e^{-\frac{t}{\theta}}$$

$$P_{max} = K_1 \left(\frac{W^{1/3}}{R} \right)^{A_1} = \text{maximum pressure (psi)}$$

$$\theta = K_2 W^{1/3} \left(\frac{W^{1/3}}{R} \right)^{A_2} = \text{time (ms) for P to decay to } \frac{P_{max}}{e}$$

where K_1, K_2, A_1, A_2 = empirical constants for a given explosive
t = time (ms)
P = pressure (psi)
R = standoff (ft)
W = charge weight (lb).

Using the empirical relationships above, a charge of 27.5 thousand tons of TNT would be required to emulate the pressure- time history generated by a 40 kT underwater nuclear explosion as illustrated in Figure 5.

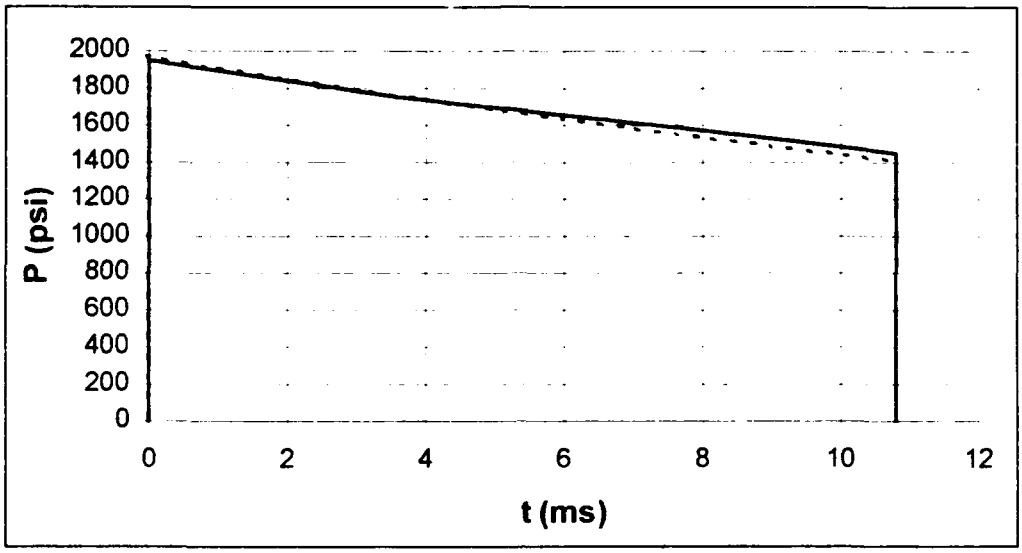

Figure 5. *Comparison of 40 kT nuclear (solid line) and 27,500 ton TNT (dashed line) explosions. R=3,000 ft, D=285 ft for both charges.*

The fact that 27.5 kT of TNT generates a similar pressure profile as a nuclear device of 40 kT yield is attributed to the thermal energy released by the nuclear explosion as discussed in Section II.A. Obviously, using 27.5 thousand tons of TNT to study the effects of a nuclear explosion is not practical, nor feasible. This amount of high explosive represents a volume greater than that of the Washington Monument (Lapp, 1980). Scaling laws, discussed in the next section, enable the use of scale models and charges of a more reasonable size to simulate the underwater nuclear explosion and its effects.

C. HOPKINSON SCALING

Dimensional analysis yields scaling principles which enable the use of scale models to replicate the behavior of full size objects, or prototypes. Of particular utility in the analysis of underwater explosions and effects is Hopkinson scaling. Through the use a scale factor λ, the quantities length, mass, and time are scaled as follows:

Model		Prototype
λL	Length	L
λt	Time	t
$\lambda^3 M$	Mass	M

giving the invariant quantities:

ρ	Density	ρ
σ, P	Stress, Pressure	σ, P
ε	Strain	ε.

Some quantities, chiefly the hydrostatic loading due to gravity, are not adaptable to scaling and require additional consideration in modeling. (Shin and Geers, 1991, §4.1)

The benefits of scaling are many. By reducing standoff and charge size, tests can be conducted in small manmade ponds with little or no environmental impact. Geometrically similar models can be constructed of the same materials as the prototype to study structural response to underwater shock. Model stress and strain levels will match those of the prototype. Since the material required to build model charges and structures is equal to λ^3 that of the prototype, model testing delivers obvious cost benefits.

Using a scale factor of λ = 1/30 to simulate the 40 kT nuclear pressure-time history discussed previously would require a spherical TNT charge of size

$$W_M = \lambda^3 W_P = \left(\frac{1}{30}\right)^3 \times 28.5 \times 10^3 \times \text{tons} \times 2{,}000\frac{\text{lbm}}{\text{ton}} = 2{,}040 \text{ lbm}.$$

The standoff required is

$$R_M = \lambda R_P = \frac{1}{30} \times 3{,}000 \text{ ft} = 100 \text{ ft}.$$

Figure 6 shows the 40 kT nuclear pressure-time history scaled using λ = 1/30 together with the pressure profile of 2,040 pounds of TNT. The only difference between this figure and Figure 5 is the time scale.

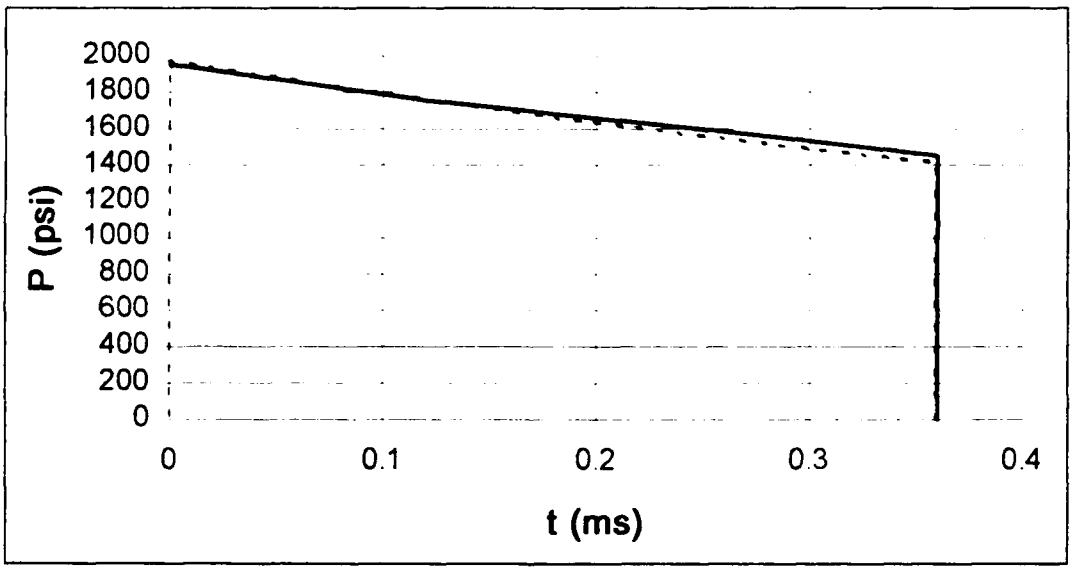

Figure 6. *2,040 lbm TNT charge (dashed line), R=100 ft, to simulate a 40 kT nuclear (solid line) explosion using a scale factor of λ = 1/30.*

Although the spherical conventional charge size is now feasible, the weight and standoff required for the simulation are too great for small pond testing limited to nominal charge weights and standoffs in the tens of pounds and feet respectively. One might be tempted in scale model testing to use a

smaller charge and shorter standoff to match only the peak pressure of the nuclear profile when studying shock effects on a scale model. As shown in Figure 7, a 14 pound spherical TNT charge at a standoff of 19 ft gives the same maximum pressure as a 2040 pound charge at a standoff of 100 ft. The pressure of the lighter charge decays much more rapidly due to its smaller time constant.

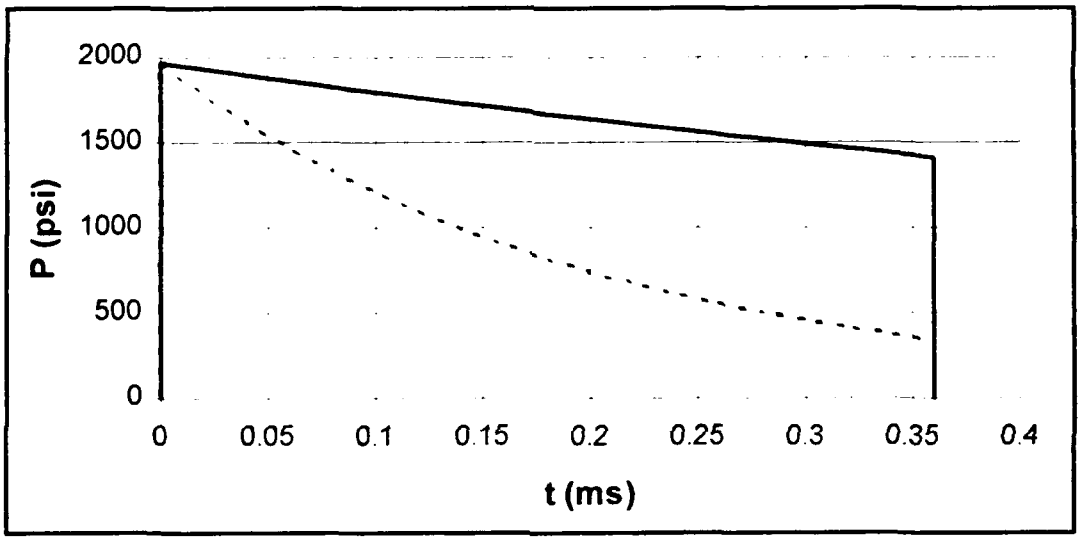

Figure 7. *Pressure-time histories of a 2,040 lbm (solid line) TNT charge at R=100 ft with a 14 lbm (dashed line) TNT charge at R=19 ft.*

It will be shown in Chapter III that the structural response from two pressure profiles having the same peak pressure but different duration of high pressure give rise to dramatically different structural responses. Therefore, in order to simulate the slow pressure decay of the underwater nuclear explosion using conventional charges of modest size, the shape of the conventional charge must be modified. The resulting shape is that of the tapered charge discussed in the next section.

D. TAPED CHARGE PRESSURE PROFILE

Designed to generate long duration shock waves to simulate nuclear underwater shock loading on scale models, tapered charges consist of a series of truncated cones on a common axis fitted with a detonator on the small or nose end as shown in Figure 8. Constructed in sizes ranging from a few ounces to over 15,000 pounds, the tapered charge generates a directional pressure field with maximum duration along the nose side on the charge axis. (Gordon and Davidson, 1983)

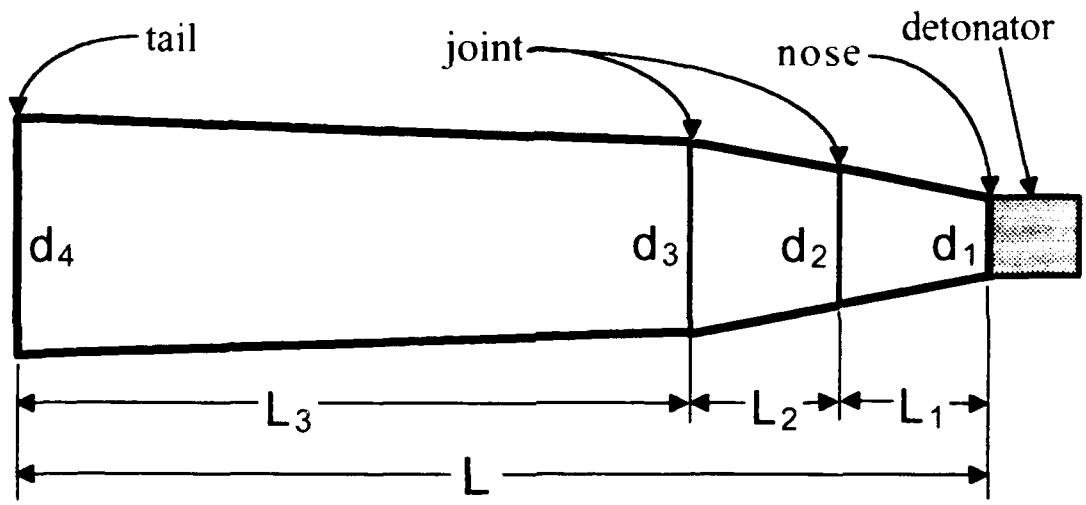

Figure 8. *Geometry of the tapered charge.*

For tapered and spherical charges of the same weight and at the same standoff, Figure 9 illustrates the trade-off between peak pressure and duration distinguishing the two designs. The tapered charge creates a peak pressure at a lower value than the spherical charge, followed by a more gradual pressure decline over a region called the pressure plateau. At the

end of the pressure plateau, the pressure-time history of the tapered charge gives way to exponential decay then surface cutoff.

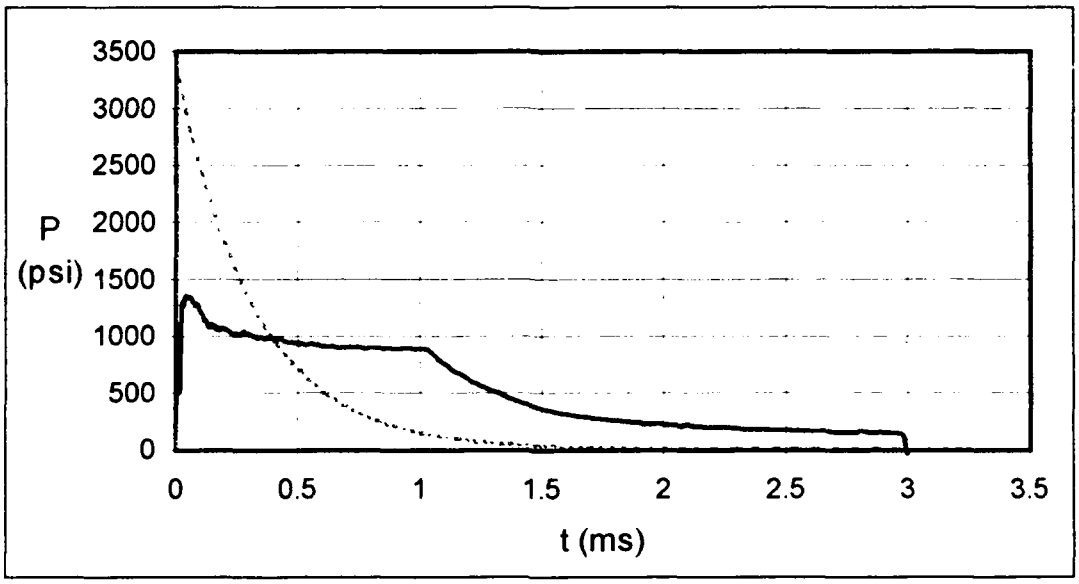

Figure 9. *Pressure profiles of tapered (solid line) and spherical (dashed line) charges with the same weight and standoff.*

The pressure plateau generated by the tapered charge gives an obvious advantage over the spherical charge in simulating the nuclear shock profile. The duration of the pressure plateau t_p can be determined to a first approximation by estimating the time difference between (1) travel from nose to tail along the charge axis a distance L at the detonation speed C_D then a distance L + R to the target at the speed of sound in water C_S, and (2) travel from the nose to the target a distance R at speed C_S. The resulting expression for pressure plateau duration is

$$t_p = \left[\frac{L}{C_D} + \frac{L+R}{C_S}\right] - \frac{R}{C_S} = L\left(\frac{1}{C_D} + \frac{1}{C_S}\right)$$

The above formula predicts a plateau duration independent of standoff. As Figure 10 shows, however, the duration of the pressure plateau actually decreases somewhat with increasing standoff.

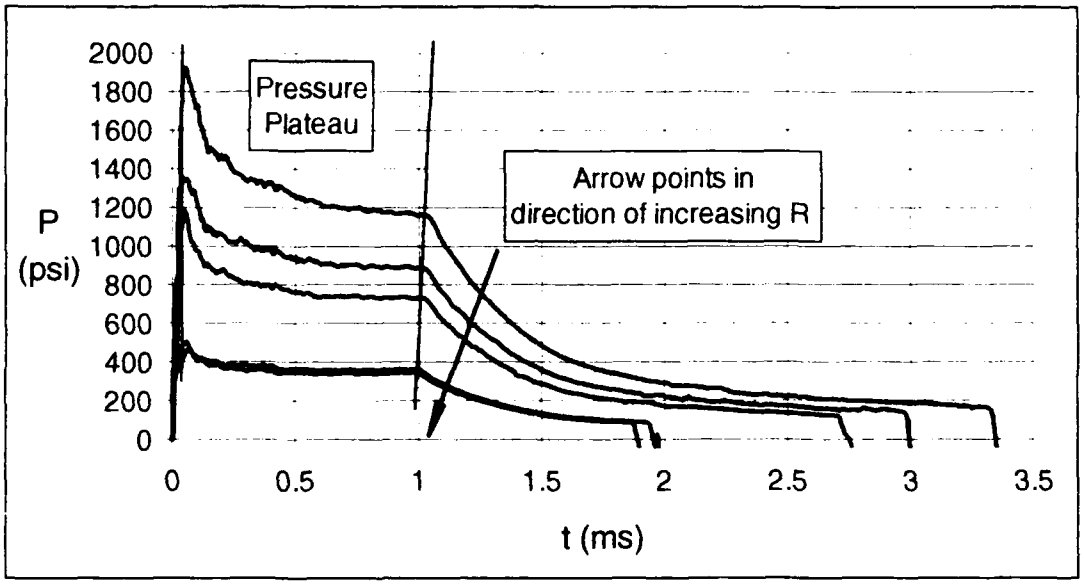

Figure 10. *Tapered charge pressure profiles at varying standoff.*

Figure 10 also shows the approximate 1/R relationship between peak pressure and standoff. In addition to varying the standoff to match peak pressures and the overall length to match pressure plateau duration, the segment lengths and diameters of the tapered charge can be varied to taylor the shape of the tapered charge pressure-time history to model a particular nuclear pressure profile. Design of a tapered charge involves first examining existing data for a charge design which produces a pressure-time history most nearly matching that desired. The charge design is then adjusted using computer calculations tempered with the experience of the designer. Small

scale experiments may be used to verify the design before production of a large tapered charge. (Costanzo, 1991)

Additional knowledge of the tapered explosion as well as any streamlining of the design process should improve the design of tapered charges used to simulate the underwater nuclear explosion. An application of the finite element method (FEM) to study the early time propagation of the shock generated by a tapered charge explosion is found in Chapter IV. Chapter V outlines the application of computer design optimization techniques to enhance the tapered charge design process.

III. EFFECT OF PRESSURE DURATION ON STRUCTURAL RESPONSE

As mentioned in Section II.C, if one could match only the peak pressure when conducting a simulation of the underwater nuclear attack, a spherical charge of modest size would suffice. As illustrated in this chapter, however, matching of peak pressures alone is not adequate. Comparison of the response of a simple cylindrical shell to side-on attack by a long duration, nuclear type, and a short duration, conventional type pressure profile yielded substantially different results using numerical techniques.

A. ATTACK CURVES

In order for a realistic comparison in the model testing environment, the pressure profiles used in this study were generated from two 56 lbm HBX-1 charges. The short duration pressure profile was derived from the empirical relationships of Section II.B for a spherical charge at a standoff of 20 ft. The long duration pressure profile used in this study to simulate the nuclear profile was derived from scaled tapered charge data. Figure 11 shows the two attack curves with the same peak pressure of approximately 3,400 psi but very different high pressure duration times. Each pressure-time history with corresponding standoff was entered into an existing computer code to provide underwater shock loading of a simple cylindrical aluminum shell model as described in the next section.

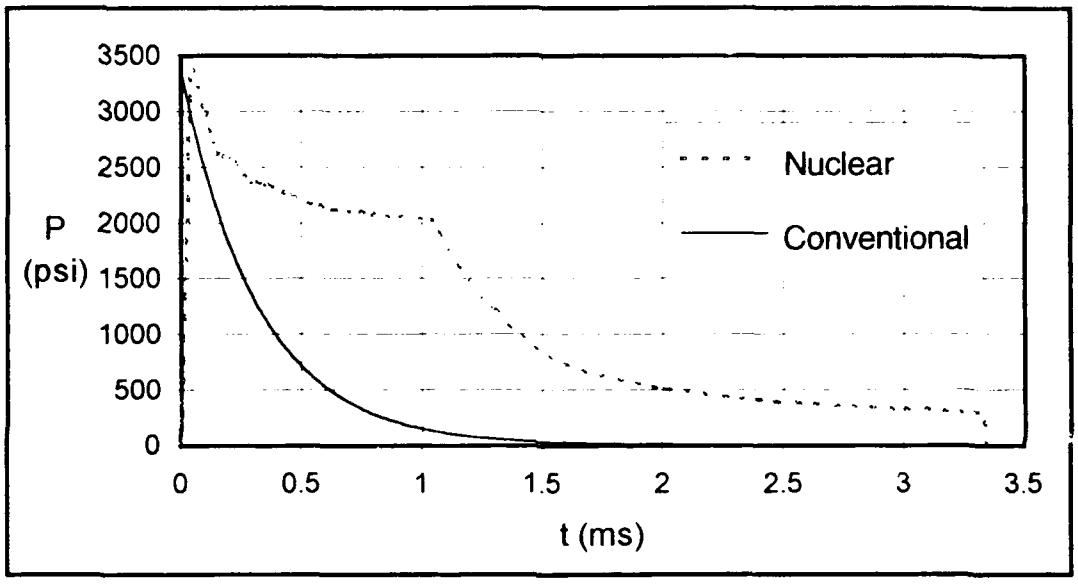

Figure 11. *Two attack curves used for comparison of structural response.*

B. NUMERICAL MODEL

The attack geometry for this study is shown in Figure 12. The figure illustrates the standoff for a spherical charge. Tapered charge standoff is, by convention, measured from the nose, Figure 8, to the target. The pressure profiles and standoffs from the previous section were used with a side-on attack cylindrical shell model developed by Fox (1992, pp. 60,61). The analysis was conducted using the public domain finite element method (FEM) code VEC/DYNA3D (Hallquist and Stillman, June, 1990) coupled with the boundary element method code USA (Deruntz, 1989). The USA (Underwater Shock Analyzer) code reduces the media surrounding the cylinder and the associated forces to discrete forces and masses to provide loading to the cylinder. The FEM code VEC/DYNA3D utilizes explicit time integration to provide the response of the cylinder to the applied shock

loading. The coupling of the two codes was initiated by the Naval Postgraduate School (Fox, Kwon, and Shin, 1992).

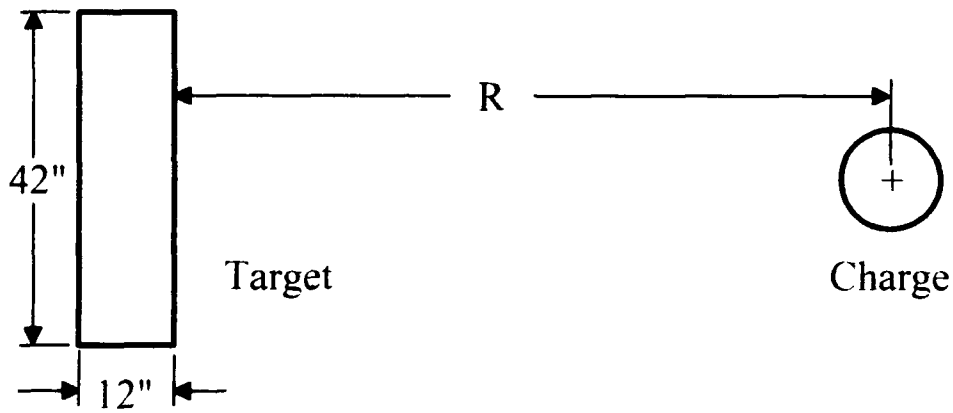

Figure 12. *Attack geometry for cylindrical shell FEM experiment.*

The target consisted of a 1/4" thick 6061-T6 aluminum cylinder with 1" machined and welded endplates. Material properties for the cylinder were:

σ_y = 40,000 psi
E = 10,800 kpsi
ν = 0.33
ρ = 174 lbm/ft^3.

Figure 13 depicts the 550 shell elements comprising the one-quarter symmetry discretization of the cylindrical shell model used in this study. A description of the theory behind the shell elements used can be found in the article by Belytschko, Lin, and Tsay (1984). Symmetric boundary conditions were applied on the yz and zx planes. The boundary element loading described previously provided the boundary conditions for the outer surface of the wet elements of the aluminum cylinder.

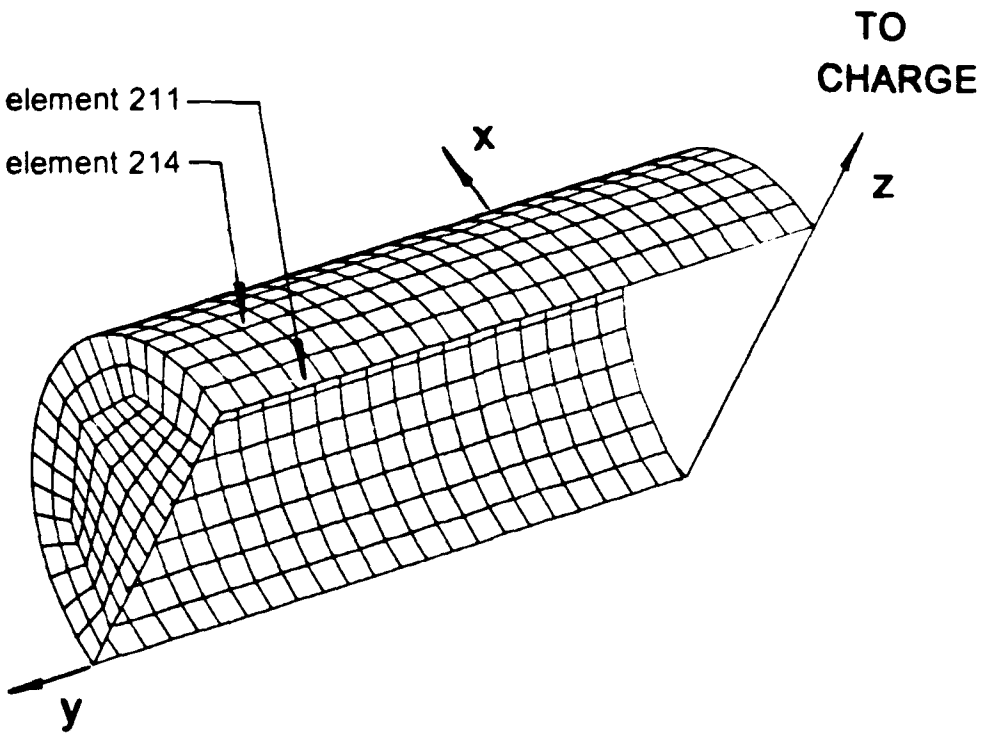

Figure 13. *Quarter symmetry FEM model of simple cylindrical shell.*

The aluminum was modeled as a kinematic/isotropic/elastic/plastic. In this idealization, elastic deformation occurs at stress levels lower than the yield stress with plastic deformation occurring at the yield stress. This provides a reasonable approximation of the uniaxial stress-strain curve for 6061-T6 aluminum based upon pull-test data as shown in Meyers and Murr (1981, p. 40), with the exception of no provision for failure once a maximum engineering strain of 7 to 9 per cent has been sustained. Taking 8 per cent plastic strain as a failure criterion and applying a factor of safety of 2, failure of the aluminum shell model was predicted for effective plastic strain in excess of 4 per cent Effective plastic strain ε_p is defined as (Ugural and Fenster, 1987):

$$\varepsilon_p = \frac{\sqrt{2}}{9}\left[\left(\varepsilon_1 - \varepsilon_2\right)^2 + \left(\varepsilon_2 - \varepsilon_3\right)^2 + \left(\varepsilon_3 - \varepsilon_1\right)^2\right]^{1/2}$$

where ε_1, ε_2, and ε_3 are the true plastic strain components. Since the maximum strain-rate calculated in this study was approximately 100 in/in-sec, well below the 2000 in/in-sec required for appreciable strain-rate effects, (Meyers and Murr, 1981, p. 50), strain-rate hardening was not included in the model.

C. RESULTS

Figures 14 and 15 show the damage sustained by the cylindrical target as a result of attack by the nuclear and conventional pressure profiles with the same peak pressures. The quarter-symmetry model has been reflected about the yz and zx planes using the post-processor TAURUS (Hallquist, 1990) to provide visualization of the full model in each case. Displacements for the conventional attack of Figure 14 were scaled by a factor of 10 to better display the damage pattern. No scaling was done in Figure 15 where the damage was much more extensive due to the nuclear type attack.

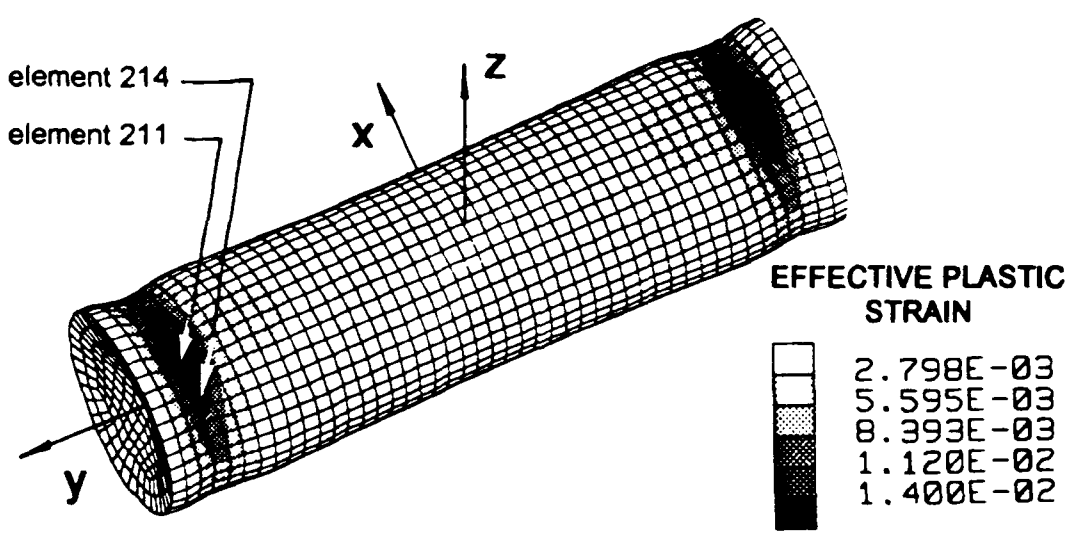

Figure 14. *Effective plastic strain from conventional attack (displacements scaled by a factor of 10).*

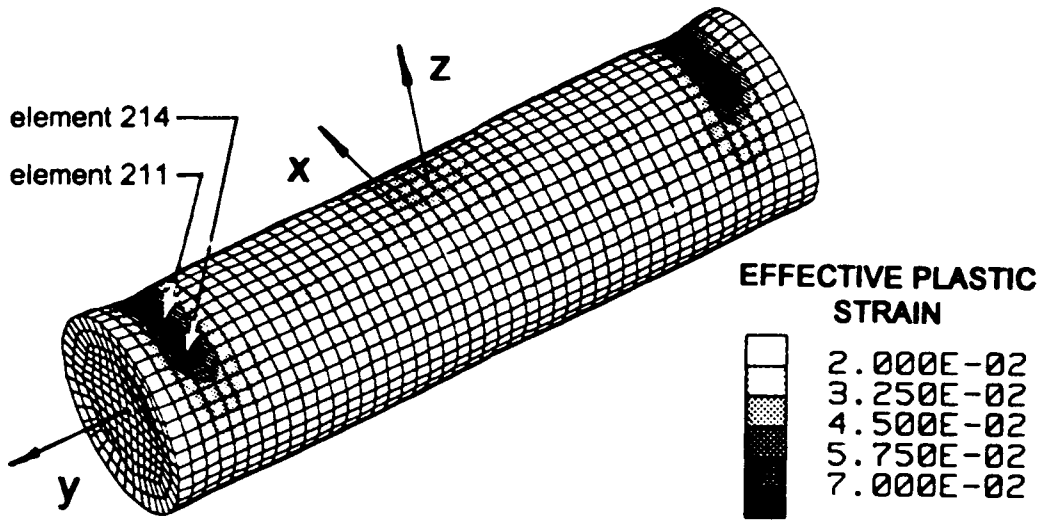

Figure 15. *Effective plastic strain from nuclear attack. (No scaling of displacements)*

Figure 16 illustrates the time history of effective plastic strain for the elements sustaining maximum damage from each attack. The maximum damage of 1.67 per cent effective plastic strain experienced by the conventional attack, although significant, did not exceed the failure criteria selected in the previous section. The effective plastic strain from the nuclear type attack, exceeding 4 per cent after less than 0.6 ms, indicates the prediction of catastrophic failure of the cylinder resulting from this attack based upon the numerical analysis.

Not only is the magnitude of effective plastic strain much greater for the nuclear type attack, the mode of damage is quite different. In both cases, maximum damage occurred in elements located approximately 3.2 inches from the endplate. In the conventional case, the maximum damage occurred in element 211, on the yz plane. Maximum damage in the nuclear case, however, occurred at element 214, 30 degrees off the yz plane.

however, occurred at element 214, 30 degrees off the yz plane. The locations of the two critical elements are shown on Figures 13 through 15.

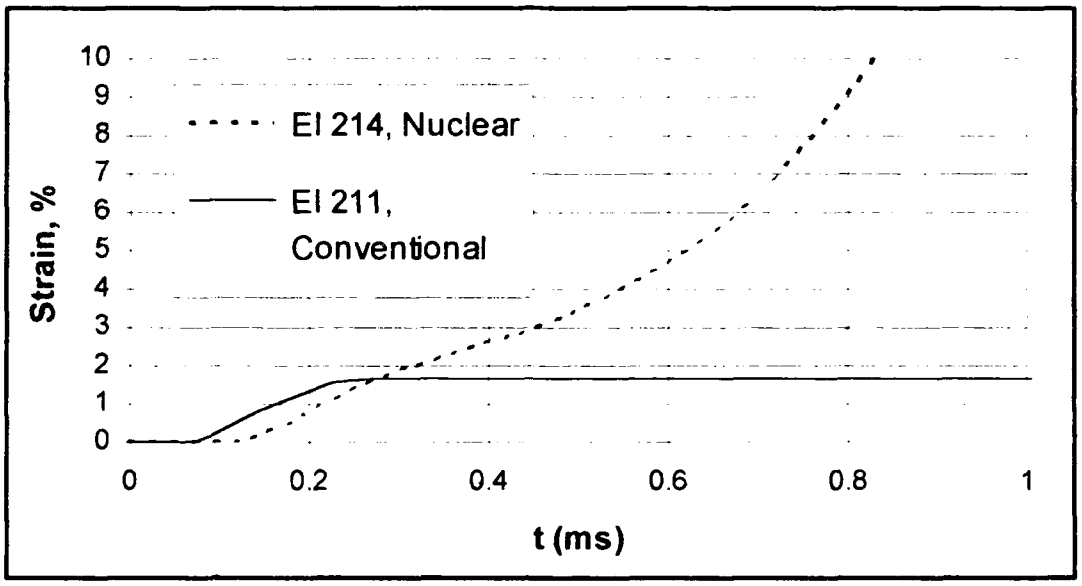

Figure 16. *Plot of effective plastic strain for the elements sustaining maximum damage.*

Based upon the analysis of this chapter, both the peak pressure and high pressure duration must be generated by the conventional high explosive used to simulate the underwater nuclear explosion. Due to the ability of the tapered charge to accomplish this task at a lower charge weight than the spherical charge, the studies of Chapters IV and V were conducted to enhance understanding and improve the tapered charge design process.

IV. THE TAPERED CHARGE SHOCK FRONT

Due to its ability to develop a long duration pressure profile from a modest charge weight, the tapered charge commonly provides the shock loading to simulate the underwater nuclear attack as discussed previously. In order to better understand the shock developed by tapered charges, finite element analysis (FEA) was conducted to study the shock developed by a tapered charge detonated underwater. The FEA provided information on the directional nature of the pressure-time history generated by the tapered charge. This information, specific for the charge geometry and type of explosive, can be used to determine the accuracy required to position the charge and target used in model studies of the underwater nuclear explosion.

A. FEA MODEL

Figure 17 shows the 46" x 46" x 152" quarter-symmetry FEA model used for this study. The mesh consists of 120 HBX-1 charge elements and 40,692 water elements. Appendix A provides a listing of the input file for the INGRID (Stillman and Hallquist, 1991) mesh generating program used. The dimensions of the tapered charge, corresponding to those of Figure 8, were:

$L_1 = L_2 = 0.333$ ft
$L_3 = 4.333$ ft
$L = 5.000$ ft
$d_1 = 1.125$ in
$d_2 = 2.625$ in
$d_3 = 4.125$ in
$d_4 = 5.375$ in.

Using a cast specific gravity for HBX-1 of 1.71 (Dobratz, 1981, p. 19.53) gives the charge weight of 60.1 lbm. Referring to Figure 17, symmetric boundary conditions were applied on the yz and zx planes. Non-reflective boundary conditions were applied to the remaining four planes.

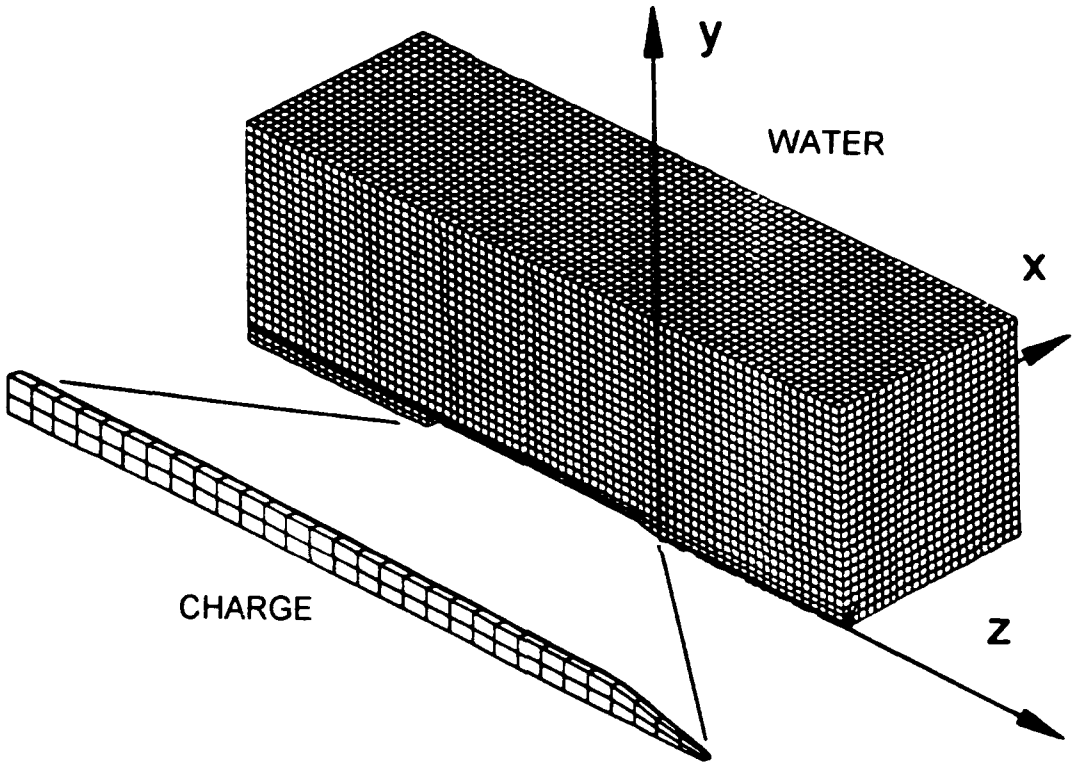

Figure 17. *FEA model used to examine the three dimensional aspects of the tapered charge.*

The charge and water model were analyzed using FEA program VEC/DYNA3D (Hallquist and Stillman, 1990). This is the stand-alone version of the coupled program used in Chapter III. The explosive was modeled as a high explosive burn material with the Jones-Wilks-Lee (JWL) equation of state, the water as a null material using the Gruneisen equation of state.

For the charge, the high explosive burn material model used by VEC/DYNA3D requires entry of the detonation velocity D, the Chapman-Jouget pressure P_{CJ}, and the density ρ (Hallquist and Stillman, 1990, p. 40). The values D = 0.731 cm/μs, P_{CJ} = 0.2204 Mbar, and ρ = 1.712 gm/cm^3 for HBX-1 were taken from Dobratz (1981, p. 19.53). The JWL equation of state was used to describe the pressure-volume-energy behavior of the detonation products (Dobratz, 1981, p. 8.21):

$$P = A(1 - \frac{\omega}{R_1 V})e^{-R_1 V} + B(1 - \frac{\omega}{R_2 V})e^{-R_2 V} + \frac{\omega E}{V}$$

Where A, B, and C = linear coefficients in Mbar
R_1, R_2, and ω = nonlinear coefficients
$V = \frac{v}{v_0} = \frac{\text{volume of detonation products}}{\text{volume of undetonated high explosive}}$
P = pressure in Mbar
E = det onation energy per unit volume in $\frac{\text{Mbar} \times \text{cm}^3}{\text{cm}^3}$.

The parameters E, A, B, R_1, R_2, and ω listed above, empirically derived from cylinder-test data, are required entries for use of the JWL equation of state with VEC/DYNA3D (Hallquist and Stillman, 1990, p. 89). For this study these values were taken from cylinder-test data for H-6, an explosive of similar composition to HBX-1, due to non-availability of HBX-1 data. The values used were (Dobratz, 1981, p. 8.22):

$E = 0.103 \frac{\text{Mbar} \times \text{cm}^3}{\text{cm}^3}$
A = 7.5807 Mbar
B = 0.08513 Mbar
R_1 = 4.9
R_2 = 1.1
ω = 0.20.

For the water, the VEC/DYNA3D null material model (Hallquist and Stillman, 1990, p. 41) requires entry of the density and an optional pressure cutoff. The value ρ = 1.000 gm/cm^3 was used for density, and a pressure cutoff value of 6.89 x 10^{-9} Mbar (0.1 psi) were used since water is unable to sustain tension. The Gruneisen equation of state with cubic shock velocity -particle velocity (u_s-u_p) defines pressure p in Kbar for compressed materials as (Hallquist and Stillman, 1990, p. 91):

$$p = \frac{\rho_0 C^2 \mu \left[1 + \left(1 - \frac{\gamma_0}{2}\right)\mu - \frac{a}{2}\mu^2 \right]}{\left[1 - \left(S_1 - 1\right)\mu - S_2 \frac{\mu^2}{\mu+1} - S_3 \frac{\mu^3}{\left(\mu+1\right)^2} \right]^2} + \left(\gamma_0 + a\mu\right) E$$

where $\mu = \frac{\rho}{\rho_0} - 1$

ρ = density in $\frac{gm}{cm^3}$

ρ_0 = standard density in $\frac{gm}{cm^3}$

and the required parameters are

C = the intercept of the u_s-u_p curve in $\frac{cm}{\mu s}$

S_1, S_2, S_3= coefficients of the slope of the u_s-u_p curve

γ_0 = the Gruneisen gamma

a = first order volume correction to γ_0.

E = internal energy per unit volume in $\frac{Mbar \times cm^3}{cm^3}$

The parameters C, S_1, S_2, and S_3, for the u_s-u_p curve were obtained from Steinberg (1987):

$$u_s = C + S_1 u_p + S_2 \frac{u_p}{u_s} u_p + S_3 \left(\frac{u_p}{u_s}\right)^2 u_p$$

$$= 0.148 + 2.56 u_p - 1.986 \frac{u_p}{u_s} u_p + 0.2268 \left(\frac{u_p}{u_s}\right)^2 u_p$$

Appendix B outlines the determination of γ_0 = 0.4934 and a = 1.3937, based upon the seventh order polynomial approximation for the Gruneisen gamma as a function of specific volume developed by Gurtman, Kirsch, and Hastings (1971).

B. RESULTS

The large number of elements led to a computationally intensive finite element analysis of the tapered charge underwater explosion. Running on a UNIX engineering workstation required approximately four days to perform the computations through 2 μs after detonation. Figure 18 shows representative time histories of two elements located at a standoff of 35" from the charge nose. One element is on the charge axis off the nose, the other 90 degrees off this axis. Due to the large variation in magnitude of pressures at the two locations, as will be shown in Section IV.B.2, the pressures have been normalized to better compare the general shapes of the curves.

The element located on the charge axis maintained a greater portion of its maximum peak pressure over a longer period of time than did the element located 90 degrees off the axis. This observation further supports the use as well as the orientation of the tapered charge for simulation of the underwater nuclear explosion.

Both of the curves of Figure 18 rose less rapidly than expected and displayed oscillatory behavior. Gordon and Davidson (1983) experienced similar results when analyzing a tapered pentolite charge using finite-difference techniques in two dimensions. They attributed the long rise time to three possible causes: the artificial viscosity coefficient built into their model, the mesh size, and the fact that their model was approximated

by a pointed nose. Although the model used in this study did not use a pointed nose approximation, the other two possible causes apply to this study. Fox (1992, pp. 9,10) cited mesh reflection effects as a contributing factor to instabilities when using the FEA code of this study.

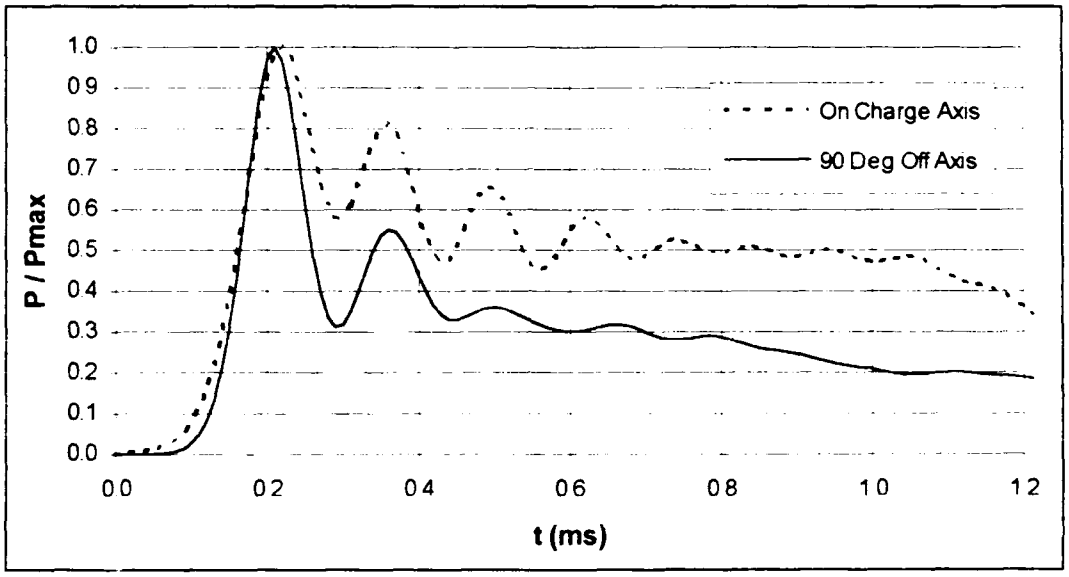

Figure 18. *Normalized Pressure-time History of two elements located at R = 45 inches: on the charge axis and 90 degrees off the charge axis.*

Although desirable, a finer mesh was beyond the capabilities of the machine used in this analysis. For this study, the default artificial viscosity coefficient and time integration steps (Hallquist and Stillman, 1990, p. 25) were used. Future sensitivity studies may identify values for these parameters. The mesh reflection effect appears to be a strong factor in the observed pressure oscillations. The key contributor to this problem, uneven size of adjacent elements, was aggravated in this study by the necessity to conform the shape of eight-node elements to the curvatures of the tapered

charge. The end result was fine charge elements near the nose next to relatively coarse water elements and a reversal of this effect at the tail of the charge.

Oscillations in pressure and the limited time of the pressure histories generated precluded determination of the pressure plateau duration. The remainder of this section concentrates on the shock wave as it emanates from the charge at early times and the directional nature of the peak pressures in the media surrounding the tapered charge.

1. Early Time Shape of the Shock Front

Figures 19 through 25 show a view perpendicular to the yz-plane of the water elements. The model has been reflected about the zx-plane, with charge elements removed. Figures 19 applies to time prior to detonation. Shading indicates the elements used for the plots of Section IV.B.2.

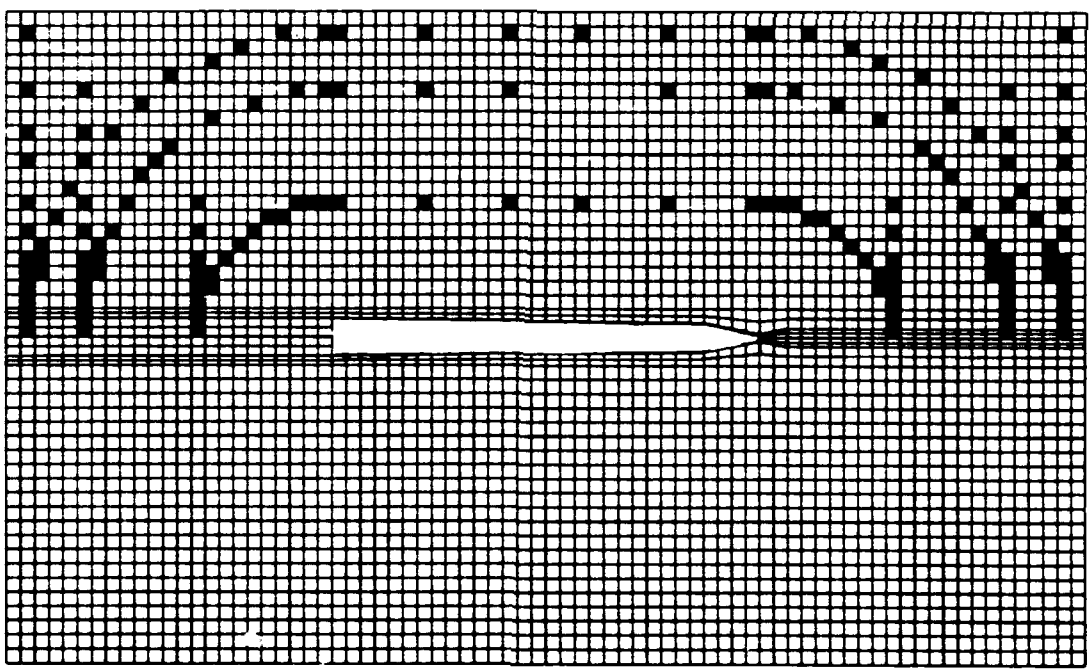

Figure 19. *Water elements prior to detonation.*

Figures 20 through 25 comprise a set of pressure contour plots at early times through 0.58 ms. There are five contour lines in each plot. The contours range from 1.000 psi for the sparsest dotted line to 5,000 psi for the solid line. This relatively low pressure range at such close proximity to the charge was selected to clearly define the location of the evolving shock.

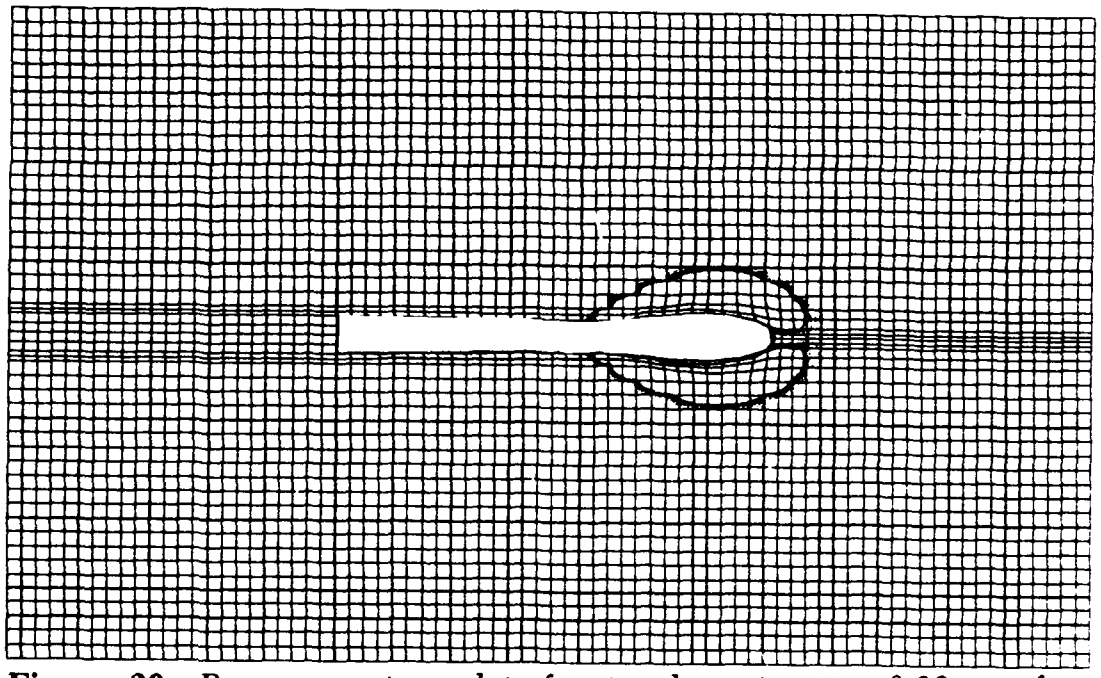

Figure 20. *Pressure contour plot of water elements at t = 0.08 ms after detonation.*

The effect of mesh reflection, discussed in the previous section, can be seen in Figure 20 along the charge axis to the front of the charge nose as the shock wave transmits through the media at different speeds in this region of very poor match of element sizes. The pressure contours bend inward toward the charge nose in the small element region. By 0.18 ms, Figure 21, the mesh reflection effect in front of the charge is negligible.

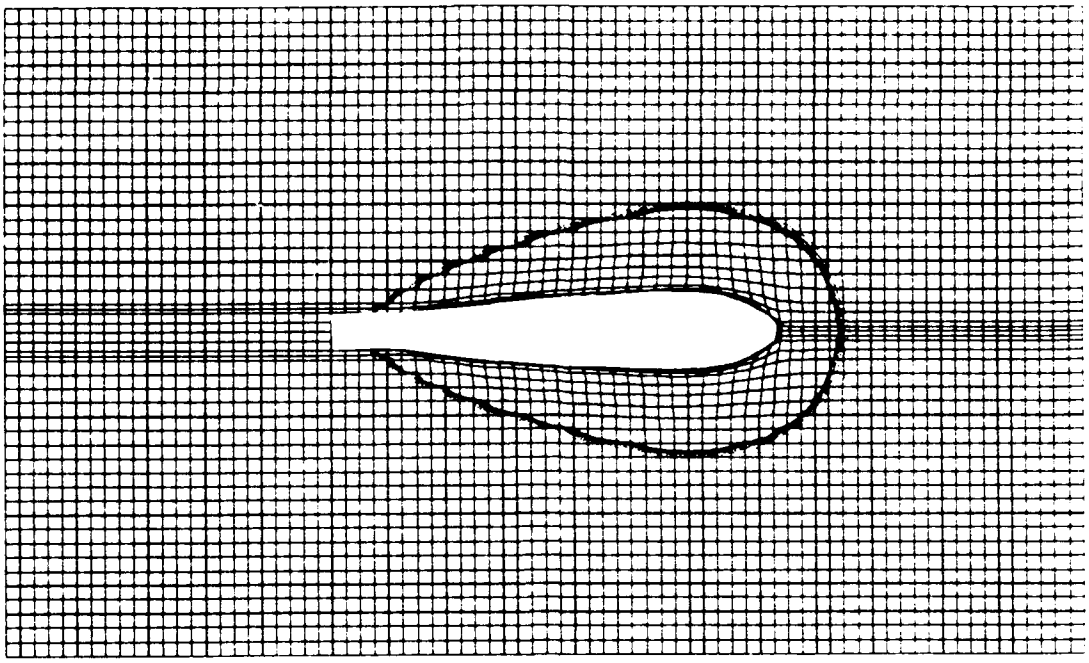

Figure 21. *Pressure contour plot of water elements at t = 0.18 ms after detonation.*

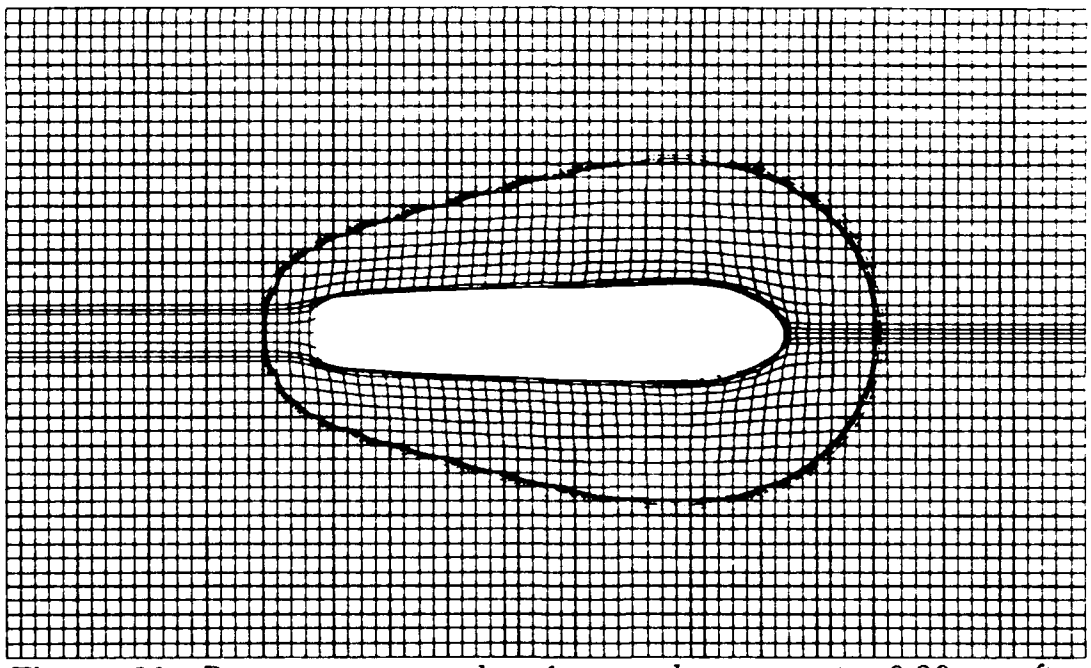

Figure 22. *Pressure contour plot of water elements at t = 0.28 ms after detonation.*

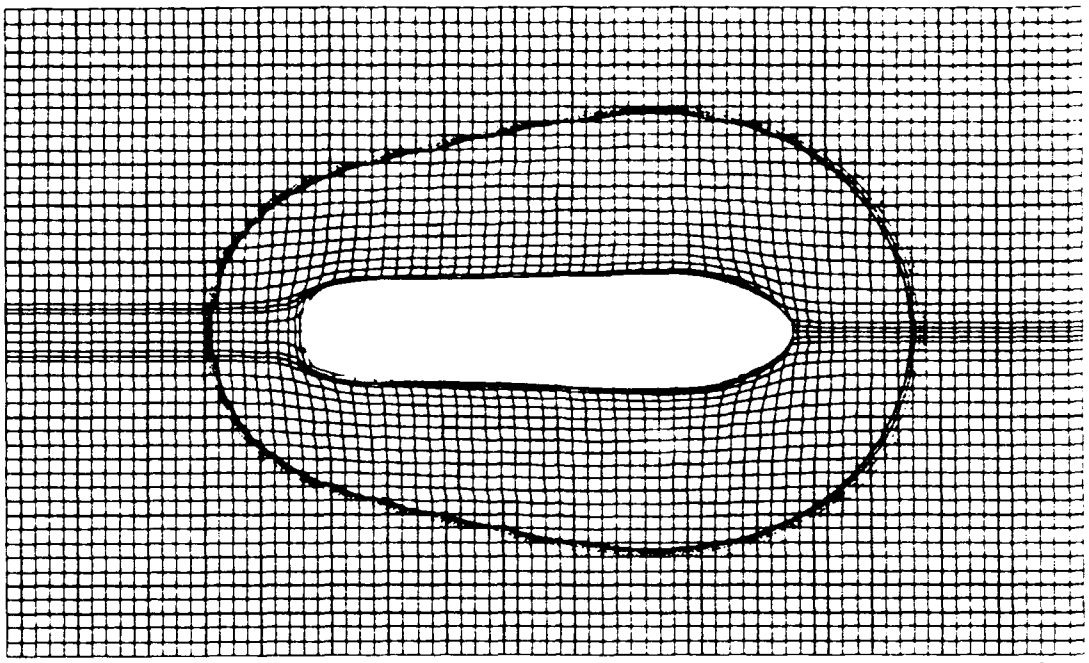

Figure 23. *Pressure contour plot of water elements at t = 0.38 ms after detonation.*

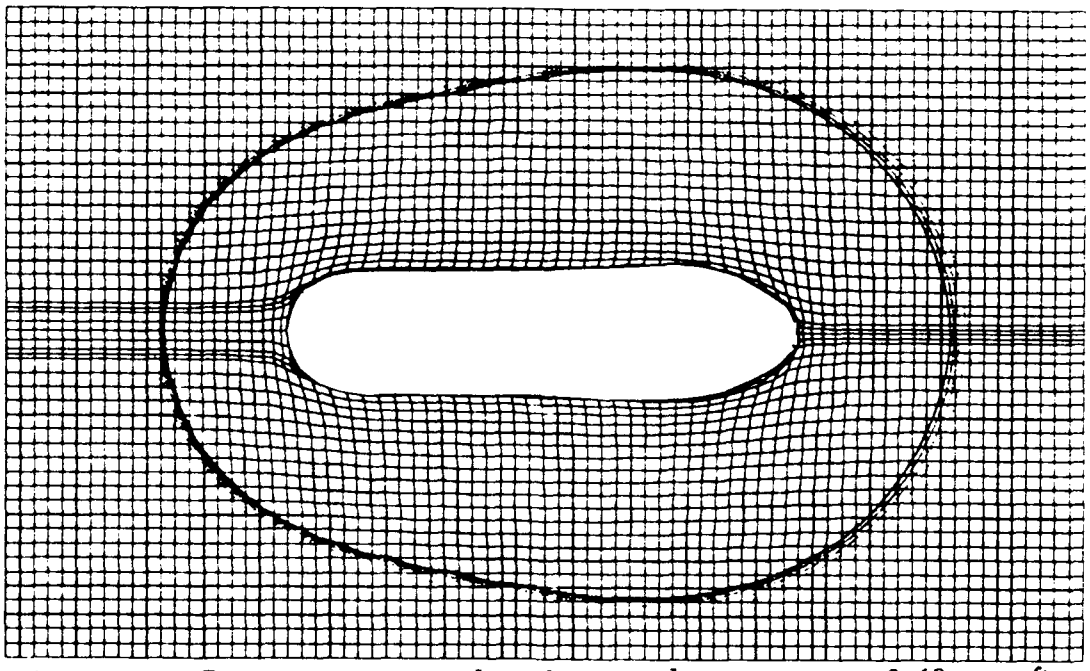

Figure 24. *Pressure contour plot of water elements at t = 0.48 ms after detonation.*

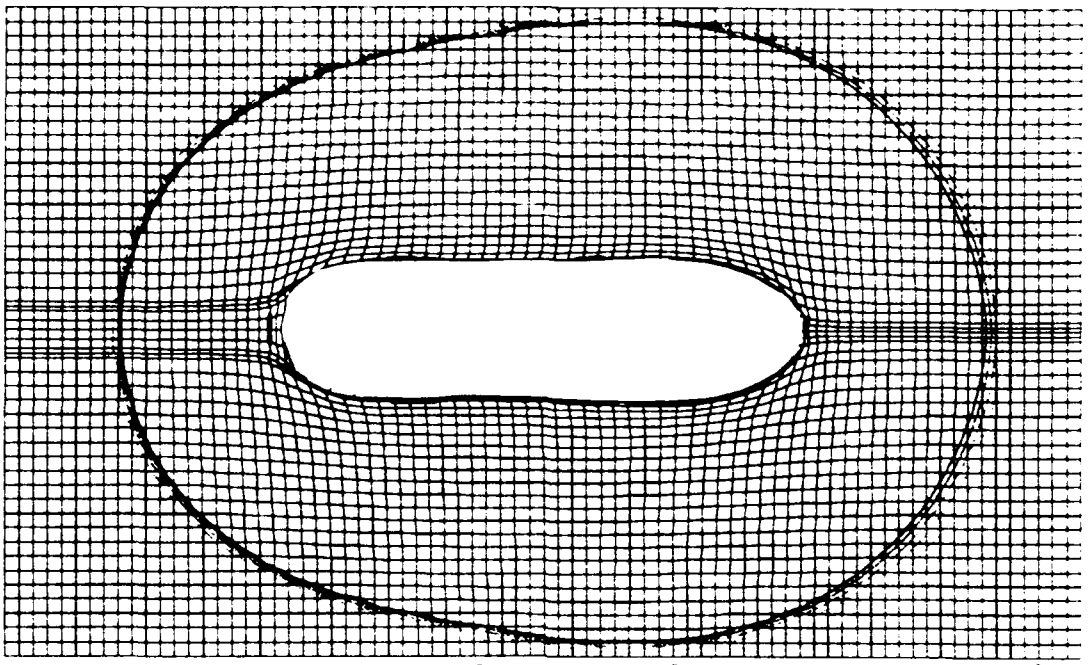

Figure 25. *Pressure contour plot of water elements at t = 0.58 ms after detonation.*

The shock front begins as a tear shape at early times emanating from the charge burn region and becoming nearly spherical on the charge axis off the nose. The above pressure contours show the nose portion of the evolving shock front to be nearly spherical in shape out to approximately 40 degrees off the charge axis with a radius centered at the location of the undetonated charge nose. Once the burn region reaches the tail of the charge, the aft portion of the shock front expands to nearly spherical with a smaller radius of curvature than at the forward end. The above figures clearly illustrate the shock rapidly travelling outward ahead of the expanding detonation products.

2. Directionality of Peak Pressure

This subsection examines variations in the peak pressure developed in regions surrounding the tapered charge based upon the FEA conducted. Figure 19 marks the locations of the elements whose pressure-time histories were gathered and processed to form the plots.

For the plots of this section, relative peak pressure P_{rel} is defined as:

$$P_{rel} = \frac{P_{max}}{P_o}$$

Where P_{max} = maximum pressure computed for the element
P_o = maximum pressure observed for the element at the same standoff and nearest the charge nose axis.

Figures accompanying the plots serve to further clarify the determination of P_{rel} as well as explain the geometry corresponding to each plot.

Figure 26 corresponds to Figure 27, a plot of relative peak pressure as a function of θ degrees off the charge nose axis from θ = 0 to 90 degrees, at constant standoff, for three different standoffs.

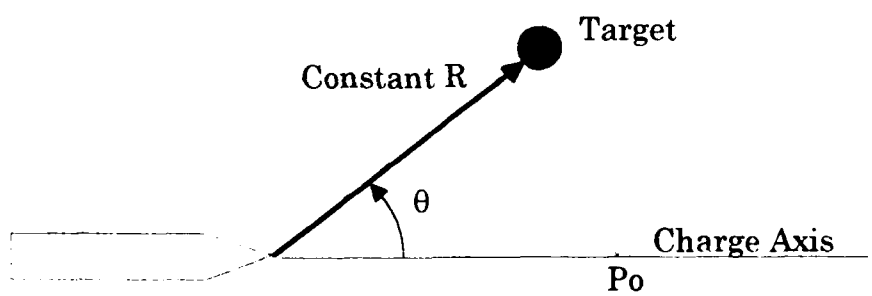

Figure 26. *Constant standoff, θ degrees off charge axis.*

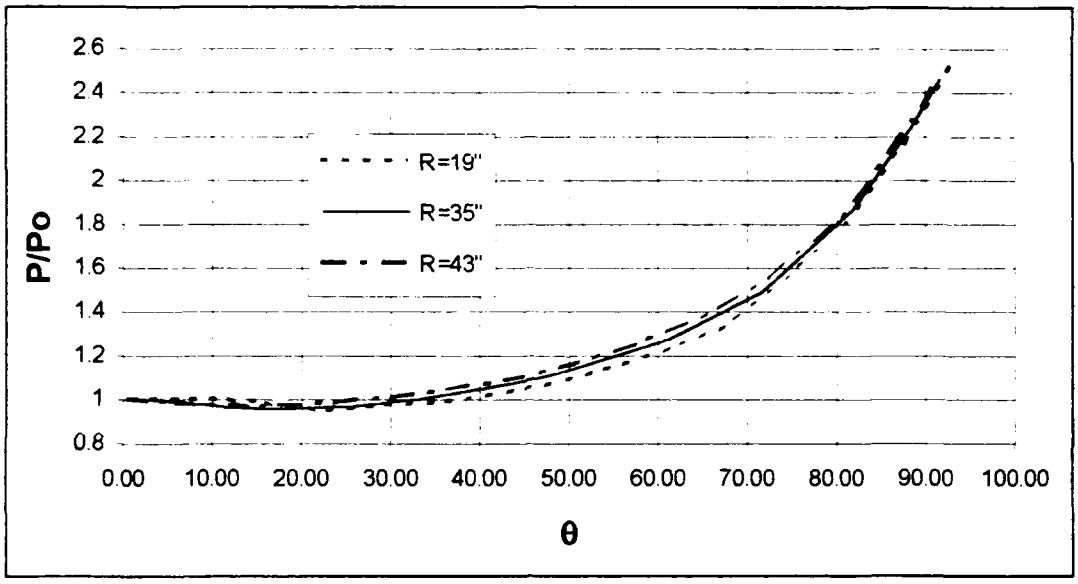

Figure 27. *Relative peak pressure as a function of the angle off the charge axis at constant standoff.*

For the three standoff distances of Figure 27, there is a decrease in pressure from the on-axis pressure as the off-axis angle increases from 0 to 20 degrees. This decrease, ranging from 3 per cent for R = 43 inches to 5 per cent for R = 15 inches, may be attributed to mesh geometry and mesh reflections. The effect of mesh geometry was caused by the centroid of each element not being at the exact standoff. This effect was minimized by applying a first order correction to each measured pressure:

$$P_R = P_{R'} \frac{R'}{R}$$

Where P_R = pressure used for plot at the nominal standoff R

$P_{R'}$ = max pressure for the given element at standoff R'

$R' = \sqrt{x^2 + y^2 + z^2}$

x, y, z = coordinates of the element centroid.

After approximately 20 degrees, the curves of Figure 27 rise steadily with increasing angle off the charge axis. This was to be expected due to the tradeoff between peak pressure duration and magnitude of the tapered charge. As θ increases, the target is placed nearer to the bulk of the mass of the charge. In a test situation gages must often be located off the charge axis to record the free-field pressure experienced by the target without being overly influenced by proximity to the target. The test designer often attempts to locate the gage as far off axis as possible while minimizing the deviation of the gage measurement from the on-axis values. Figure 27 indicate that, for the charge and standoffs of this study, gages could be located up to 35 degrees off the charge axis for an error in maximum peak pressure measurement of less than 5 per cent. To keep the error in measurement of plateau duration to an acceptable level, the allowable off-axis angle may lie well below the level based upon peak pressure alone.

Past 90 degrees off the front charge axis, constant standoff was replaced by constant distance y off the charge axis to examine the relative pressures experienced by elements to the side of the charge. Figure 28 illustrates the geometry involved. P_o for this case is taken at a standoff R = y on the axis off the charge nose as shown in the figure. Figure 29 shows relative peak pressure as a function of ξ / L off the charge axis for ξ / L = 0 to 1 from nose to tail. As can be seen from the figure, relative peak pressure shows marked departure for different values of y. While the highest relative peak pressure occurred at ξ / L = 0.8, the magnitude fell from 8.4 at y = 19 inches to 6.2 at y = 43 inches. This was likely a close-in phenomenon. It is

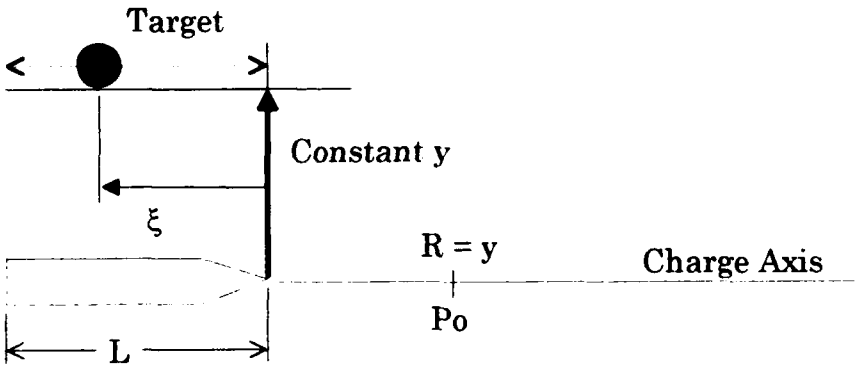

Figure 28. *Constant distance off the charge axis, to the side of the charge.*

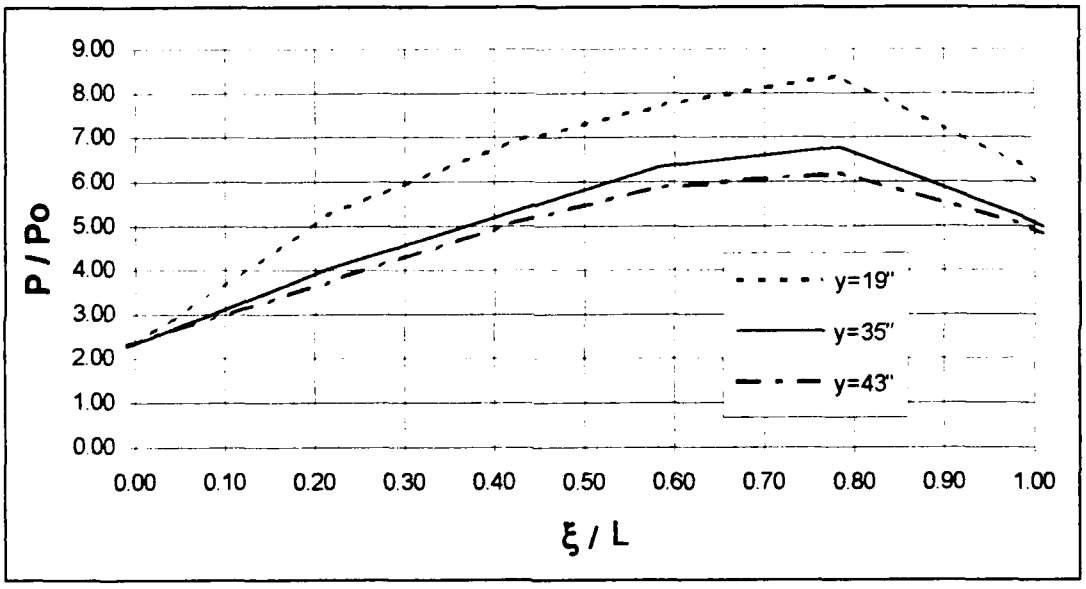

Figure 29. *Relative peak pressure as a function of the fraction of the length aft of the nose at constant distance off the charge axis to the side.*

expected that, at distances further removed from the charge axis than those of this study, the maximum relative peak pressure to the side of the charge will continue to fall then reach a steady value significantly lower than calculated here. Of interest is the fact that the maximum relative peak

pressure observed for elements located to the side of the charge was found at ξ / L = 0.8, significantly aft of the center of gravity location at ξ / L = 0.6. This may be due to a build-up in pressure away from the center of gravity location in the direction of the tapered charge high explosive burn.

Completing the examination of pressures encircling the charge from fore to aft, Figure 30 shows the geometry corresponding to Figure 31 plotting the variation in relative peak pressure at a constant standoff R measured from the center of the tail. The angle θ in this case is measured from 90 degrees off the rear charge axis toward the rear charge axis in order to continue proceeding in a counterclockwise direction. As in the two other cases, P_o is measured off the charge nose, in this case at a standoff equal to the constant R. As in the constant R case off the charge nose, a correction was applied to the calculated values to account for variation in standoff of the element centroids.

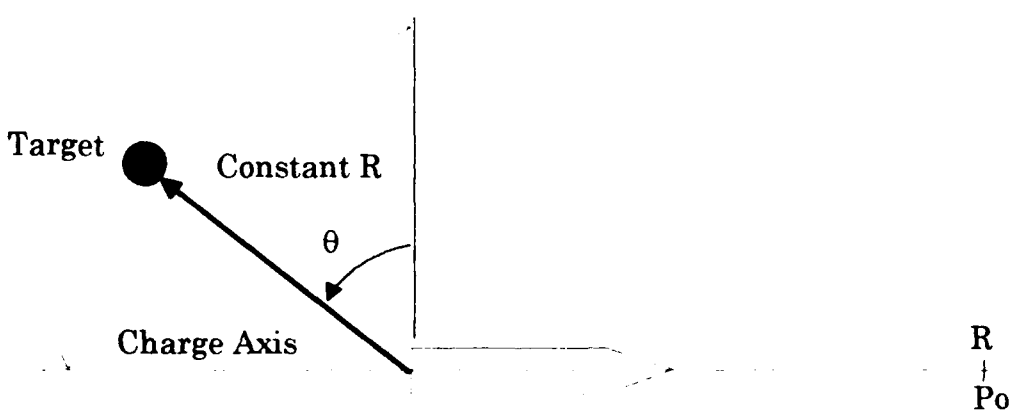

Figure 30. *Constant R off the rear charge axis.*

Figure 31 shows a continuation of the decrease in peak pressure for the standoffs studied until θ = 60 degrees, or 30 degrees off the charge tail

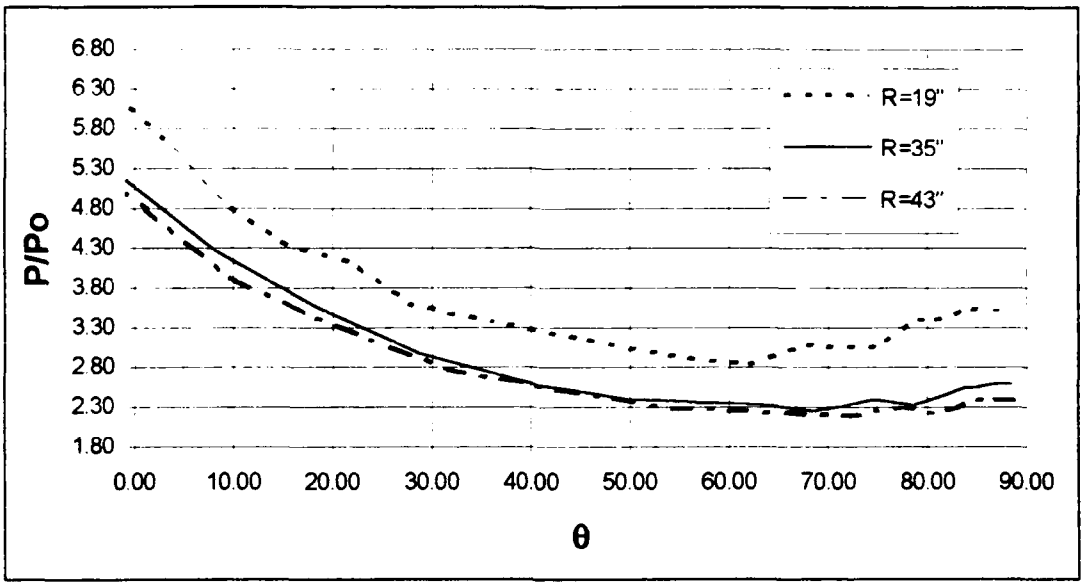

Figure 31. *Relative peak pressure as a function of degrees aft of the charge.*

axis followed by a slight increase to the charge axis. Here again, the unevenness of the curves near the axis may be attributed in part to mesh reflections. As in the side case, the relative pressure curves, though exhibiting similar shape, varried significantly for different standoffs, with shorter standoff corresponding to higher relative peak pressure. Though of minor interest in nuclear simmulations, the side and rear relative pressure plots are of more interest to weapons and industrial high explosive designers. The higher pressures at the tail end of the charge agree with the use of this configuration for demolition and other applications.

Of more interest in simulations is the effect of distance off axis at a constant standoff from the charge nose as illustrated in Figure 32. This configuration, somewhat easier to set up for experimental verification, yielded the plot of Figure 33 which provides information of similar utility as the constant R plot of Figure 27.

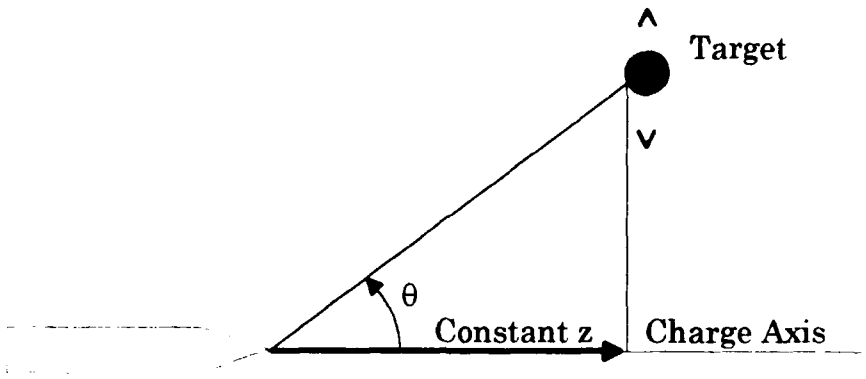

Figure 32. *Constant distance from nose along charge axis.*

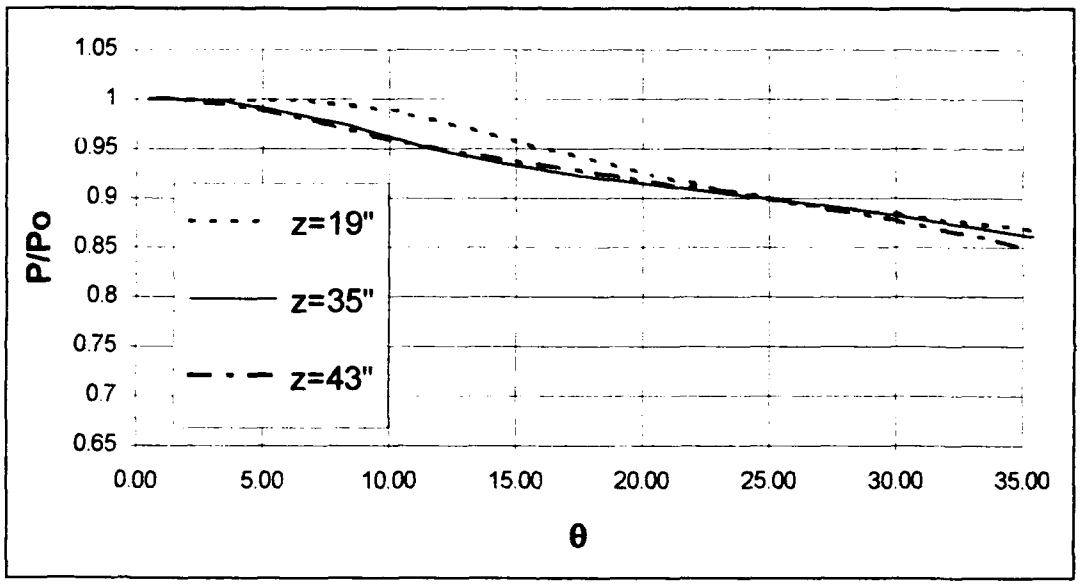

Figure 33. *Relative peak pressure at constant distance along charge axis as a function of degrees off the charge axis.*

Figure 33 indicates that, for the studied charge design and stand off distances, the off axis distance may be varied up to 10 degrees before exceeding a 5 per cent error in peak pressure readings. Since the allowable angle to stay within a given error tolerence decreased with range, a smaller angle would be allowed at the longer ranges used in simulations of the

underwater nuclear explosion. Having concluded the FEA of the underwater tapered charge explosion. the next chapter outlines computer optimization of a simple method to determine the pressure-time history of a tapered charge.

V. TAPERED CHARGE DESIGN OPTIMIZATION

This chapter outlines the coupling of a public domain computer optimization package ADS (Vanderplaats, 1984) and a simple tapered charge pressure-time generating program TAPER (Costanzo, 1991) to optimize the tapered charge design process. The coupling program, listed in its entirety in Appendix C, can be used with existing and future tapered charge pressure-time history generating codes to enhance the design of the tapered charges used to simulate underwater nuclear explosions.

In addition to the program in Appendix C, ADS (Automated Design Synthesis) and a pressure-time generating subroutine are required to perform tapered charge design optimization.

A. SIMPLE PRESSURE-TIME HISTORY ALGORITHM

Simpler, less computationally intensive, computer codes than that used for the finite element analysis of the previous chapter exist to predict the pressure profile of an underwater tapered charge explosion. These simpler codes are usually based upon an empirically based superposition principle.

Because the empirically based exponential approximation of Chapter II works well for spherical / near spherical charges, one method of deriving the pressure-time history of an underwater tapered charge explosion is to partition the tapered charge into subsegments as shown in Figure 34. Each subsegment is considered to be a separate charge generating its own pressure-time history. (Costanzo, 1991)

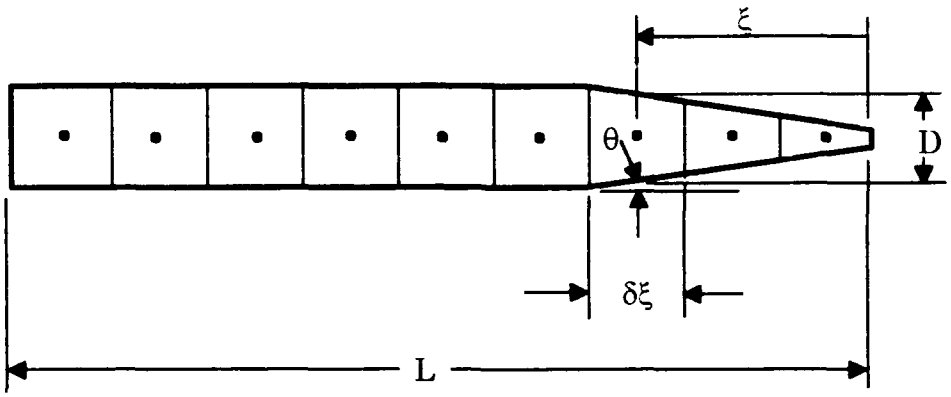

Figure 34. *Tapered charge discretized into subsegments for calculation of pressure-time history using summation method.*

Shocks generated by subsegments detonated after the nose subsegment travel in shocked media at faster speeds than preceding shocks, overtaking them. There is thus a summation or stacking effect of individual "wavelets" to determine the overall pressure-time history of the tapered charge underwater explosion (Costanzo, 1991):

$$P = \sum_{i=1}^{N} \frac{A_i}{r_i} e^{-\frac{Bt}{D_i}} \delta\xi$$

Where
- P = pressure as a function of time
- N = number of waves stacked
- A_i = empirical amplification factor, a function of θ_i
- θ_i = slope angle of subsegment
- $r_i = R + \xi_i$ = subsegment standoff
- R = standoff from charge nose to target
- ξ = distance from nose to subsegment midpoint
- B = empirical decay constant
- t = time
- D_i = charge diameter at subsegment midpoint
- $\delta\xi$ = subsegment length.

Figure 35 illustrates the superposition scheme for a simple tapered charge discretized into large segments.

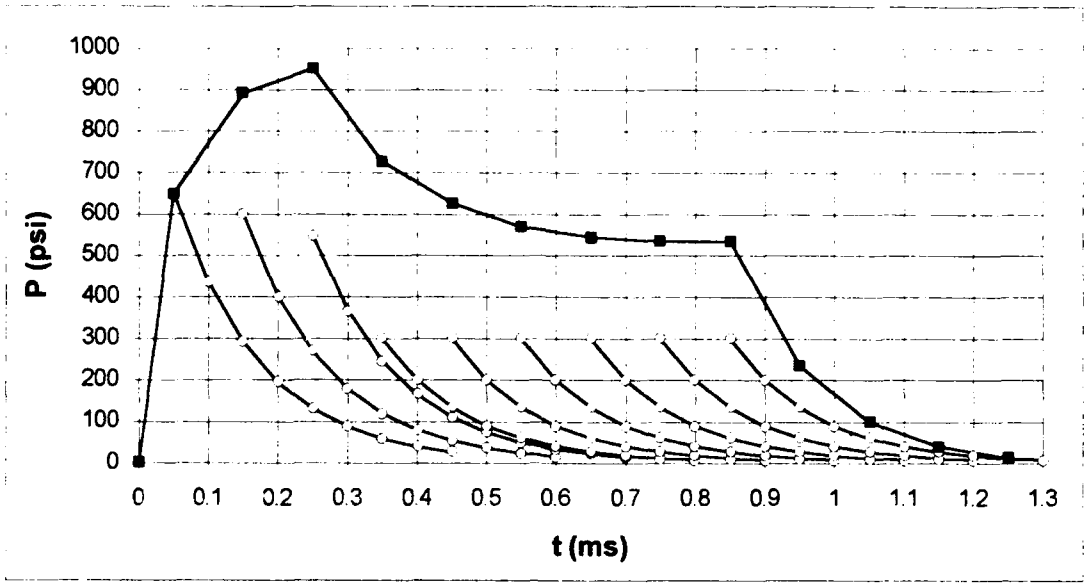

Figure 35. *Summation of wavelets generated by charge subsegments to obtain resultant pressure-time history for a tapered charge.*

One algorithm, using a superposition scheme and empirical data to determine the pressure-time history of a tapered charge detonated underwater is the PASCAL program TAPER written by Fred Costanzo (1991). This program was converted to a FORTRAN program then to the FORTRAN subroutine used for tapered charge design optimization. Besides a basic overhaul of the input / output, a simple provision for surface cutout was added to the original algorithm.

B. OPTIMIZATION PROBLEM

The objective of the tapered charge design optimization was to determine charge geometry, as depicted in Figure 8, and standoff required to develop a pressure-time history most nearly matching a desired pressure-time history. The average square root of the sum of the squares of the differences between the computed and desired pressures at each time

increment was selected to quantify the difference between the optimal design and desired pressure profiles. Constraints restricted the charge to increasing diameters and placed upper and lower limits on charge weight, charge dimensions, and standoff. Only designs within these limits were allowed. For a tapered charge of three segments, the optimization problem became:

$$\text{minimize:} \quad \sqrt{\sum_{i=1}^{N} \frac{\left(P_i - p_i\right)^2}{K}}, \qquad i = 1, N$$

$$\begin{aligned} \text{subject to:} \quad & 1 \text{ in} < L_i < 20 \text{ ft}, && i = 1 \text{ to } 3 \\ & 0.75 \text{ in} < d_i < 10 \text{ in}, && i = 1 \text{ to } 4 \\ & 5 \text{ ft} < R < 30 \text{ ft}, \\ & 25 \text{ lbm} < W < 125 \text{ lbm}, \\ & d_1 < d_2 < d_3 < d_4 \end{aligned}$$

where
N = number of computed pressure-time history points
P_i = desired pressure at a particular time
p_i = computed pressure at a particular time
L_i = charge segment length
d_i = charge joint diameter
R = standoff
W = charge weight.

The main FORTRAN program DTAPOPT was written to accomplish the tapered charge design optimization using, as described previously, the ADS optimization package and the subroutine based upon the TAPER program.

C. OPTIMIZATION PROGRAM

In addition to DTAPOPT, three subroutines for use in conjunction with the main program were also written. The first, DCOMPAR, computes the square root of the average sum of the squares of the pressure differences. The second, DPTGEN, interpolates to find the desired pressure

corresponding to the design pressure at a given time. This subroutine enables the comparison of the desired and design pressures at the same times. The third subroutine, DTAPWT, computes the weight of the tapered charge for evaluation of the weight constraint.

1. Required Program Input

DTAPOPT requires input from two files and the keyboard. Figure 36 shows a sample of a tapin.dat file used to input initial charge geometry, standoff, nominal length of pressure-time history to be computed, and surface cutoff time. Decimal alignment and horizontal placement on the lines is optional with one number per line only. Number translations have been written into the figure.

3	*number of charge segments*
0.5	*length of first segment (ft)*
1.0	*length of second segment (ft)*
5.0	*length of third segment (ft)*
1.0	*first joint, or nose, diameter (in)*
2.0	*second joint diameter (in)*
3.0	*third joint diameter (in)*
5.0	*fourth joint, tail, diameter (in)*
15.1	*standoff (ft)*
1.12	*nominal length of computed time history (ms)*
1.095	*surface cutoff time (ms)*

Figure 36. *Sample tapin.dat file. Italics, not part of the file, indicate the meaning of each number.*

Figure 37 shows a sample of the second input file, profin.dat, used to input the desired pressure profile for program DTAPOPT. Up to 1001 data points may be entered without program modification. The first time entered must be at time zero, and the last time must be greater than the nominal length of computed time history entered in tapin.dat. Decimal alignment

and horizontal placement on the lines is optional. Only one number can be used on the first line, two on the rest. Number translations added to the figure are shown in italics.

9		*ndes, total number of desired pressure-time data points minus 1*	
0.0	0.0	*tdes(0) in ms--must be zero.*	*pdes(0) in psi*
0.04	1950.0	*tdes(1)*	*pdes(1)*
0.119	1755.0	*tdes(2)*	*pdes(2)*
0.278	1560.0	*tdes(3)*	*pdes(3)*
0.417	1365.0	*tdes(4)*	*pdes(4)*
0.635	1170.0	*tdes(5)*	*pdes(5)*
0.834	975.0	*tdes(6)*	*pdes(6)*
1.072	780.0	*tdes(7)*	*pdes(7)*
1.120	0.0	*tdes(8)*	*pdes(8)*
3.0	0.0	*tdes(9)*	*pdes(9)*
tdes(ndes) must be greater than nominal length of p-t history entered in tapin.dat			

Figure 37. *Portion of a sample profin.dat file. Italics, not part of the file, have been added to indicate what each number represents.*

Three integers comprise required keyboard input. These numbers control the optimization method used by ADS. Vanderplaats (1985) provides more detailed instruction on method selection. Vanderplaats (1984) provides the theory behind the methods. The three numbers consist of any one number from each of three groups. The first number may be any of the following to determining the optimization strategy:

First Number	Optimization Strategy
0	Go directly to the optimizer
6	Sequential Linear Programming
7	Method of Centers (Design must be feasible)
8	Sequential Quadratic Programming
9	Sequential Convex Programming.

The second required input number may be either of the following to determine the optimizer:

Second Number	Optimizer
4	Method of Feasible Directions
5	Modified Method of Feasible Directions.

The last input number, one of the following, selects the one-dimensional search option to be used:

Third Number	One-Dimensional Search
5	Golden Section Method
6	Golden Section Method Plus Polynomial Interpolation
7	Bounded Polynomial Interpolation
8	Unbounded Polynomial Interpolation.

2. Program Output

Output from DTAPOPT includes one screen summarizing the optimization and an output file containing the design and interpolated desired pressure-time histories.

Figure 38 shows a sample screen from a run of DTAPOPT on a personal computer. The figure shows the execution commands followed by prompts for the three inputs, in this case the user selected the combination 8-5-7 for the strategy, optimizer, and search. The output summary then lists the initial and final charge designs as well as the average square root of the pressure differences for each case and the number of calls to the pressure-time generating routine.

```
C:\P&C\FOR\OPT:dtapopt

 ENTER ISTRAT.IOPT,IONED:  8 5 7

      INITIAL DESIGN
        LENGTHS =          1.000     1.000     5.000          FT
        DIAMETERS =        1.00      2.00      4.00      5.00 IN
        CHARGE WEIGHT =  66.0 LB
        RANGE =          20.0 FT
        SQRT OF AVG OF (Pdesign-Pdesired)^2 = 424.3 PSI

      FINAL DESIGN
        LENGTHS =          0.083     0.083     4.825          FT
        DIAMETERS =        2.52      3.75      4.28      4.52 IN
        CHARGE WEIGHT =  55.7 LB
        RANGE =          17.4 FT
        SQRT OF AVG OF (Pdesign-Pdesired)^2 = 240.3 PSI

      CALLS TO P-T HISTORY GENERATOR = 158

C:\P&C\FOR\OPT:
```

Figure 38. *Sample screen output from DTAPOPT.*

The output screen of Figure 38 represents an early step in the design process. The next would be to use this final design to input a more refined initial design, then run the optimization program again. For test optimizations. the square root of the average pressure difference squared was well below 100 for the "best" final design.

Figure 39 shows a portion of a sample DTAPOPT output file. The first two columns contain the calculated time and pressure, the third column contains the interpolated values of the desired pressure profile input. The data are in free format to retain maximum precision, sacrificing the readability of formatting. This output file may be readily used to create plots comparing the initial and final designs as was done in the next section of this chapter.

```
0.00000000000000000E-01 0.00000000000000000E-01 0.00000000000000000E-01
2.81022269002981981E-02  1639.32749805998742000  1405.11134501490983000
5.62044538005963962E-02  1675.89437624031484000  1987.35262142392480000
          .                        .                        .
          .                        .                        .
          .                        .                        .
  0.47773785730506935  1628.10858635031309000  1658.35094063994575000
  0.50584008420536752  1614.83610147863396000  1636.41749525434739000
  0.53394231110566581  1602.96393658242482000  1614.48404986874857000
          .                        .                        .
          .                        .                        .
          .                        .                        .
  1.06788462221133162   900.78633515776994000   899.17511224684437800
  1.09598684911162980 0.00000000000000000E-01   235.12876911529235700
```

Figure 39. *Sample excerpted from an output data file generated by DTAPOPT.*

D. OPTIMIZATION RESULTS

The design space using the subroutine adapted from program TAPER proved to be fraught with local minima attributable discontinuities resulting from integer changes in the number of waves stacked. Several runs of DTAPOPT using different optimization methods for a particular initial design resulted in an improved design unless the initial design was optimal. The improved design was then used as the initial design for further optimization. This process was repeated from four to seven times until further optimizations failed to improve the design an appreciable amount. Each run of DTAPOPT took approximately two minutes on a personal computer of modest, 386SX, capacity. Total time to perform a tapered charge design optimization was from one to two hours.

Of the desired pressure profiles and initial designs tested, input parameter combinations 0-5-7, 8-5-7, and 9-5-7, usually produced the most improved design with the fewest calls to the pressure-time history generating

subroutine. These input numbers translate, as shown in Section V.C.1 to direct optimization, sequential quadratic programming, or sequential convex programming strategy combined with the modified method of feasible directions optimizer and a bounded polynomial interpolation one-dimensional search. For the best designs found, as mentioned in Section V.C.2, the square root of the average difference between desired and design pressures was well below 100 psi. Figure 40 shows a comparison of the pressure profile generated by an optimized design from program DTAPOPT and the corresponding desired pressure profile.

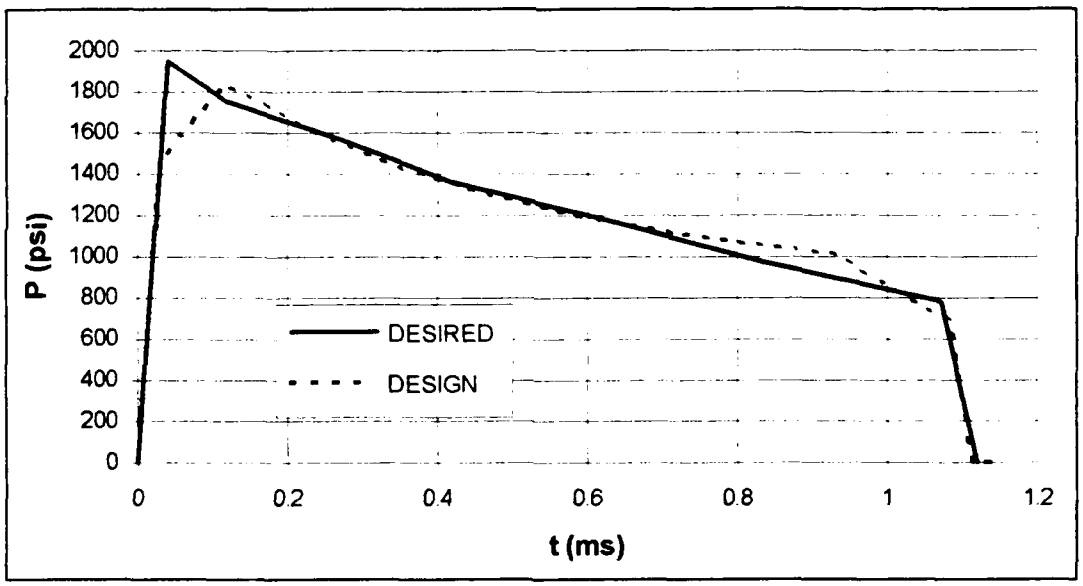

Figure 40. *Pressure profile resulting from optimization compared with the corresponding desired pressure profile.*

VI. CONCLUSIONS AND RECOMMENDATIONS

The boundary element / finite element analysis of the side on attack of a simple cylinder by nuclear and conventional type pressure profiles resulted in substantially different structural responses. It is therefore necessary to model the duration of the pressure plateau to adequately simulate structural response to an underwater nuclear explosion.

The finite element analysis of an underwater tapered charge explosion provided insight to the early time propagation of the shock wave and the directional variations in peak pressures developed in the surrounding media. There is need for future research, including sensitivity studies of the artificial viscosity coefficient and the time integration step, to obtain less oscillatory results to provide tapered charge pressure plateau duration information. Additionally, the computationally intensive method used lends itself more readily to supercomputer use where the mesh size may be extended far enough away from the charge form comparison with test data.

Coupling of an optimization routine with a tapered charge pressure profile generating routine provides a tool which can be used to more efficiently design tapered charges used to simulate underwater nuclear explosions. The program written for this study may be used with existing and future pressure-time history codes.

APPENDIX A: TAPERED CHARGE FEM INPUT FILE

Following is a complete listing of the input file used to perform FEM analysis on the tapered charge and water model of Chapter IV:

```
GOGO2

c Set up for DYNA3D, integrate to time 2000, TAURUS data dump interval
10,
c  high speed printer dump interval 29999.

 dn3d vec term 2000 plti 10.0 prti 29999.0

c Scale x, y, z axes from inches to cm.

 xsca 2.54 ysca 2.54 zsca 2.54

c Define material 1, type 8--High explosive burn, HBX-1:
c  detonation vel 0.731 cm/us, Chapman-Jouget pres 0.2204 Mbar,
c  density 1.712 gm/cc.

 mat 1 type 8 d .731 pcj .2204 ro 1.712

c Equation of state for charge: 2--JWL:
c  a 7.5807, b .08513, r1 4.90, r2 1.10, omega .20, e0 .103 Mbar-cc/cc.

 eos 2 a 7.5807 b .08513 r1 4.90 r2 1.10 omega 0.20 e0 0.103 endmat

c Define material 2, type 9--Null Material, Water:
c  cutout pressure .1 psi (6.89e-9 Mbar), density @ 4 deg C 1.000 gm/cc.

 mat 2 type 9 pc 6.89e-9 ro 1.000

c Equation of state for water: 4--Gruneisen:
c  sound speed .142 cm/us @ 4 deg C, s1 2.56, s2 -1.986, s3 .2268,
c  Gruneisen gamma .4934, first order vol cor'n to gamma 1.3937.

 eos 4 sp .142 s1 2.56 s2 -1.986 s3 0.2268 gamma .4934 sa 1.3937 endmat

c Define two symmetry planes by defining a point and a normal vector
c  for each plane.  Any point within .001 cm of a symmetry plane will be

c  included in that plane's definition.

 plane 2
  0 0 0  1 0 0 .001 symm
  0 0 0  0 1 0 .001 symm

c Define detonation points in HBX-1.

 detp 1 point 0 0 0;
```

```
c Define rear and front water cylinders, cone and plane surfaces for
c  charge nose (part 1) and transition water (part 2).

 sd 1 cn2p 0 0  0  0 0 1   0.5625       0.0  1.3125       -4.0
 sd 3 plan 0 0  0  0 0 1
 sd 4 plan 0 0 -4  0 0 1

c Part 1: small charge cone.

start
 1 3 5;
 1 3 5;
 1 3;
 -1 0 1
 -1 0 1
 0.0 -4.0
 di 1 0 3; 1 0 3; ;
 sfi  -1 -3; -1 -3; ; sd 1
 sfi  -1 -3; -1 -3; -1 -1; sd 3
 sfi  -1 -3; -1 -3; -2 -2; sd 4
 d 1 1 1  2 3 2
 d 1 1 1  3 2 2
 mate 1
end

c Part 2:  water transition from small charge cone to square grid.

start
 1 3 5 7 9;
 1 3 5 7 9;
 1 3;
 -4 -4 0 4 4
 -4 -4 0 4 4
 0.0 -4.0
 di 1 2 0 4 5 ; 1 2 0 4 5 ; ;
 d 2 2 0  4 4 0
 sfi  -2 -4 ; -2 -4 ; ; sd 1
 sfi  -1 -5 ; -1 -5 ; -1 -1 ; sd 3
 sfi  -1 -5 ; -1 -5 ; -2 -2 ; sd 4
 d 1 1 1  3 5 2
 d 1 1 1  5 3 2
 mate 2
end

c Define cone and plane surfs for med charge and transition (pts 3 and
4).

 sd 8  plan 0 0 -8  0 0 1
 sd 9  cn2p 0 0  0  0 0 1   1.3125       -4.0   2.0625       -8.0

c Part 3: medium charge cone.

start
 1 3 5;
 1 3 5;
 1 3;
 -1 0 1
 -1 0 1
 -4.0 -8.0
```

```
 di 1 0 3; 1 0 3; ;
 sfi  -1 -3; -1 -3; ; sd 9
 sfi  -1 -3; -1 -3; -1 -1; sd 4
 sfi  -1 -3; -1 -3; -2 -2; sd 8
 d 1 1 1  2 3 2
 d 1 1 1  3 2 2
 mate 1
end

c Part 4: medium water transition.

start 1 3 5 7 9;
 1 3 5 7 9;
 1 3;
 -4 -4 0 4 4
 -4 -4 0 4 4
 -4.0 -8.0
 di 1 2 0 4 5 ; 1 2 0 4 5 ; ;
 d 2 2 0  4 4 0
 sfi  -2 -4 ; -2 -4 ; ; sd 9
 sfi  -1 -5 ; -1 -5 ; -1 -1 ; sd 4
 sfi  -1 -5 ; -1 -5 ; -2 -2 ; sd 8
 d 1 1 1  3 5 2
 d 1 1 1  5 3 2
 mate 2
end

c Define cones and plane for large charge and transition (pts 5 and 6).

 sd 11 cn2p 0 0   0   0 0 1   2.0625       -8.0   2.6875       -60.0
 sd 13 plan 0 0 -60   0 0 1

c Part 5: large charge cone.

start
 1 3 5;
 1 3 5;
 1 27;
 -1 0 1
 -1 0 1
 -8.0 -60.0
 di 1 0 3; 1 0 3; ;
 sfi  -1 -3; -1 -3; ; sd 11
 sfi  -1 -3; -1 -3; -1 -1; sd 8
 sfi  -1 -3; -1 -3; -2 -2; sd 13
 d 1 1 1  2 3 2
 d 1 1 1  3 2 2
 mate 1
end

c Part 6: large water transition.

start
 1 3 5 7 9;
 1 3 5 7 9;
 1 27;
 -4 -4 0 4 4
 -4 -4 0 4 4
 -8.0 -60.0
 di 1 2 0 4 5 ; 1 2 0 4 5 ; ;
```

```
 d 2 2 0  4 4 0
 sfi  -2 -4 : -2 -4 : : sd 11
 sfi  -1 -5 ; -1 -5 ; -1 -1 ; sd 8
 sfi  -1 -5 : -1 -5 : -2 -2 : sd 13
 d 1 1 1  3 5 2
 d 1 1 1  5 3 2
 mate 2
end

c Define cylinders for front and rear water cylinders and transitions.

 sd cl cyli 0 0 0  0 0 1   2.6875

c Part 7: rear water cylinder.

start
 1 3 5:
 1 3 5:
 1 24:
 -1 0 1
 -1 0 1
 -60.0 -106.0
 di 1 0 3: 1 0 3: :
 sfi  -1 -3: -1 -3: : sd cl
 sfi  -1 -3: -1 -3; -1 -1: sd 13
 d 1 1 1  2 3 2
 d 1 1 1  3 2 2
 nrb 0 0 2  0 0 2
 mate 2
end

c Part 8: rear water transition.

start
 1 3 5 7 9:
 1 3 5 7 9:
 1 24:
 -4 -4 0 4 4
 -4 -4 0 4 4
 -60.0 -106.0
 di 1 2 0 4 5: 1 2 0 4 5 : :
 d 2 2 0 4 4 0
 sf 2 2 1  4 4 2  sd cl
 sfi -1 -5: -1 -5: -1 -1: sd 13
 d  1 1 1  3 5 2
 d  1 1 1  5 3 2
 nrb 0 0 2  0 0 2
 mate 2
end

c Define cones and plane for water cone and transition (parts 9 and 10).

 sd 5 cn2p 0 0  0   0 0 1   0.5625       0.0   1.3125        4.0
 sd 7 plan 0 0  4   0 0 1

c Part 9: front water cone.

start
 1 3 5;
 1 3 5;
```

```
 1 3;
 -1 0 1
 -1 0 1
  0.0 4.0
 di 1 0 3; 1 0 3 ; ;
 sfi  -1 -3; -1 -3; ; sd 5
 sfi  -1 -3; -1 -3; -1 -1; sd 3
 sfi  -1 -3; -1 -3; -2 -2; sd 7
 d 1 1 1  2 3 2
 d 1 1 1  3 2 2
 mate 2
end

c Part 10: front water cone transition.

start
 1 3 5 7 9;
 1 3 5 7 9;
 1 3;
 -4 -4 0 4 4
 -4 -4 0 4 4
 0.0 4.0
 di 1 2 0 4 5 ; 1 2 0 4 5 ; ;
 d 2 2 0  4 4 0
 sfi  -2 -4; -2 -4; ; sd 5
 sfi  -1 -5; -1 -5; -1 -1; sd 3
 sfi  -1 -5; -1 -5; -2 -2; sd 7
 d  1 1 1  3 5 2
 d  1 1 1  5 3 2
 mate 2
end

c Define cylinder for front water, parts 11 and 12.

sd c2 cyli 0 0 0  0 0 1   1.3125

c Part 11: front water cylinder.

start
 1 3 5;
 1 3 5;
 1 22;
 -1 0 1
 -1 0 1
 4.0 46.0
 di 1 0 3; 1 0 3; ;
 sfi -1 -3; -1 -3; ; sd c2
 sfi -1 -3; -1 -3; -1 -1; sd 7
 d 1 1 1  2 3 2
 d 1 1 1  3 2 2
 nrb 0 0 2  0 0 2
 mate 2
end

c Part 12: front water cylinder transition.

start
 1 3 5 7 9;
 1 3 5 7 9;
 1 22;
```

```
 -4 -4 0 4 4
 -4 -4 0 4 4
 4.0 46.0
 di 1 2 0 4 5; 1 2 0 4 5 ; ;
 d 2 2 0 4 4 0
 sf 2 2 1  4 4 2  sd c2
 sfi -1 -5; -1 -5; -1 -1; sd 7
 d  1 1 1  3 5 2
 d  1 1 1  5 3 2
 nrb 0 0 2  0 0 2
 mate 2
end

c Part 13: top water.

start
 1 24;
 1 22;
 1  24 54 77;
 0.0 46.0
 4.0 46.0
 -106.0 -60.0  0.0 46.0
 nrb 2 0 0  2 0 0
 nrb 0 2 0  0 2 0
 nrb 0 0 1  0 0 1
 nrb 0 0 4  0 0 4
 mate 2
end

c Part 14: side water.

start
 1 22;
 1  3;
 1  24 54 77;
 4.0 46.0
 0.0  4.0
 -106.0 -60.0  0.0 46.0
 nrb 2 0 0  2 0 0
 nrb 0 0 1  0 0 1
 nrb 0 0 4  0 0 4
 mate 2
end

end
```

APPENDIX B: GRUNEISEN GAMMA APPROXIMATION

The seventh order approximation for the Gruneisen gamma as a function of the specific volume v developed by Gurtman, Kirsch, and Hastings (1971) is:

$$\gamma(v) = a_0 + a_1 v + a_2 v^2 + \cdots + a_7 v^7$$

where
$a_0 = 2,366.6324$
$a_1 = -22,669.420$
$a_2 = 91,259.368$
$a_3 = -200,175.85$
$a_4 = 258,585.11$
$a_5 = -196,872.84$
$a_6 = 81,850.023$
$a_7 = -14,342.530$
γ = Gruneisen gamma, dimensionless
v = specific volume in $\frac{cm^3}{gm}$.

By definition,

$$\mu = \frac{\rho}{\rho_0} - 1 = \frac{v_0}{v} - 1$$

giving $$v = \frac{v_0}{\mu + 1} = \frac{1}{\mu + 1} \text{ for } \rho = 1 \frac{g}{cm^3} = \frac{1}{v_0}.$$

Substituting $1/(\mu+1)$ for v into the Gurtman equation for $\mu = 0$ to 0.8 in .001 increments, then using a least squares linear fit with the same intercept resulted in the following linear equation for $\gamma(\mu)$:

$$\gamma(\mu) = \gamma_0 + a\gamma = 0.4934 + 1.3937\mu$$

Figure 41 is a plot of $\gamma(\mu)$ from the Gurtman equation and the linear approximation.

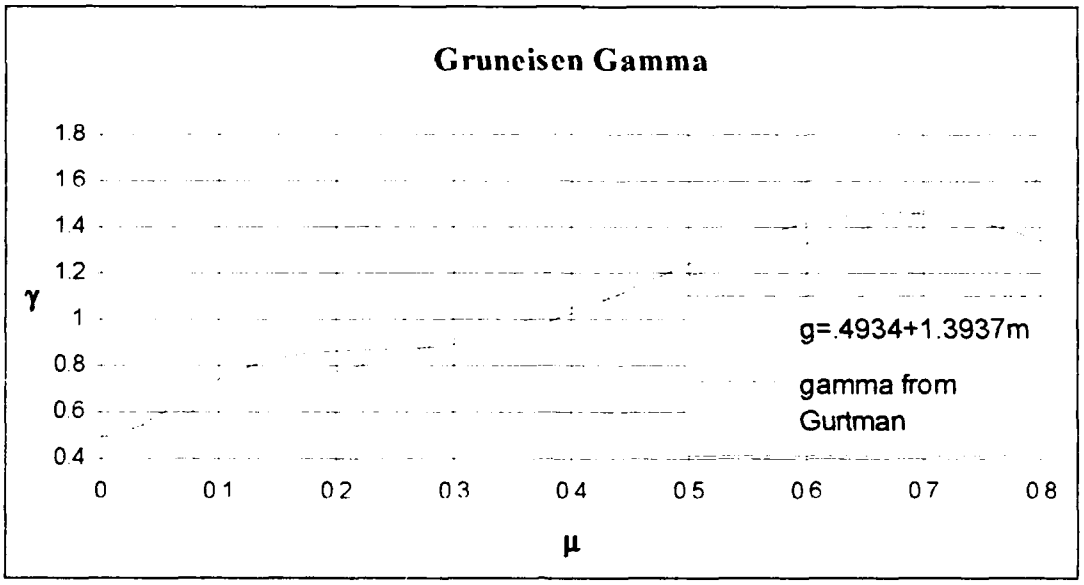

Figure 41. *Comparison of $\gamma(\mu)$ from Gurtman, Kirsch, and Hastings equation with the linearized equation for $\gamma(\mu)$.*

APPENDIX C: FORTRAN PROGRAM

This appendix contains a complete listing of the FORTRAN main program DTAPOPT and its supporting subroutines DCOMPAR, DPTGEN, and DTAPWT, written to optimize tapered charge design. A separate subroutine to generate pressure-time histories given tapered charge geometry and standoff distance is required, as well as the optimization package ADS.

PROGRAMMING NOTE: The program DTAPOPT and associated subroutines were written in double precision FORTRAN. The public domain version of ADS is written in single precision. ADS was converted to double precision for use with DTAPOPT. DTAPOPT and its three subroutines can be simply converted to single precision by removing the IMPLICIT NONE and DOUBLE PRECISION statements from the codes.

I. PROGRAM DTAPOPT

```
c     DTAPOPT
c          This FORTRAN program combined with subroutines DCOMPAR,
c     DPTGEN, and DTAPWT, is designed to optimize tapered charge design
c     using the public domain optimization package ADS (converted to
c     DOUBLE PRECISION by the author)
c          --When coupled with a separate subroutine (not included)
c     to calculate the pressure-time history of a three-segment tapered
c     charge.
c          Up to ten charge segments may be used with appropriate
c     modifications to the input files.
c - - - - - - - - - - - - - - - - - - - - - - - - - - - - - - - - - - - - -
c     PRECISION:              DOUBLE
c     INPUT FILES:            TAPIN.DAT  Initial Design.
c                             PROFIN.DAT Desired P-T History.
c     INTERRACTIVE INPUT:     Optimization options.
c     OUTPUT FILE:            Named in TAPIN.DAT, plot data for computed
c      time vs computed pressure and interpolated pressure.
c     SCREEN OUTPUT:          Starting and Optimized Designs.
c     REQUIRED SUBROUTINES:   DTAPWT  Computes charge weight.
c                             DPTGEN  Linearly interpolates to give desired
```

```
c     pressure at each time output by P-T history generator.
c                          DCOMPAR Computes the square root of the
c     average of the square of the difference between the computed and
c     interpolated desired pressure at each time.
c                          ADS     Package of subroutines which perform
c     the optimization.
c                          P-T HISTORY GENERATOR.
c    AUTHOR:               William Earl Miller II
c    MOST RECENT UPDATE:   6/16/92
c    REFERENCES:           (1) Vanderplaats, G. N., ADS - A FORTRAN
c     Program for Automated Design Synthesis, Version 1.10, program
c     instructions, Naval Postgraduate School, Montery, California,
c     May, 1985.
c                          (2) Vanderplaats, G. N., Numerical
c     Optimization Techniques for Engineering Design:  With Applica-
c     tions, McGraw-Hill Publishing Company, 1984.
c    TEST P-T GENERATOR:   The subroutine SDTAPER, was converted to
c    FORTRAN by the author, based upon the PASCAL program TAPER version
c    7/27/89 by F. A. Costanzo.
c - - - - - - - - - - - - - - - - - - - - - - - - - - - - - - - - - - - -
c    DATA INPUT FILES--Two required:
c      TAPIN.DAT contains 12 lines, one value per line which are read
c      into the program.  The integer and decimal data need only be in
c      a format suitable for list-directed input assignment to INTEGER
c      and DOUBLE PRECISION data types respectively.  The character data
c      must be in proper form for a DOS file name.
c       LINE                                          READ TO       DATA
c      NUMBER          DESCRIPTION                   VARIABLE       TYPE
c        1     number of charge segments              NTAP        integer
c        2     length of charge segment (ft)         TAP(1)       decimal
c        3                 "                         TAP(2)       decimal
c        4                 "                         TAP(3)       decimal
c        5     diameter of charge segment (in)       DIAM(1)      decimal
c        6                 "                         DIAM(2)      decimal
c        7                 "                         DIAM(3)      decimal
c        8                 "                         DIAM(4)      decimal
c        9     standoff (ft)                          RANGE       decimal
c       10     nominal length of time history (ms)   TLEN        decimal
c               used by P-T generating subroutine
c       11     pressure cutout time (ms)              TCO         decimal
c               used by P-T generating subroutine
c       12     name of output data file to be        NAMFIL      character
c               created
c      PROFIN.DAT contains NDES+2 lines, one integer value (NDES) on the
c      first line, two decimal values on each of the remaining lines.
c      Times must be in ascending order starting with 0.0 and extending
c      to a time greater than TLEN entered in TAPIN.DAT above.
c    LINE                                          READ TO          DATA
c   NUMBER          DESCRIPTION                   VARIABLE          TYPE
c      1   total number of desired pressure-        NDES           integer
c           time history data pairs minus one
c      2   first time   first pressure       TDES(0) PDES(0)       decimal
c        (must be zero)
c      3   second time  second pressure      TDES(1) PDES(1)       decimal
c      .                .                          .                .
c      .                .                          .                .
c      .                .                          .                .
c    NDES+2  NDES time  NDES pressure    TDES(NDES) PDES(NDES) decimal
c - - - - - - - - - - - - - - - - - - - - - - - - - - - - - - - - - - - -
c    INTERRACTIVE KEYBOARD INPUT--three integers required
```

```
c    These integers control the optimization method used by ADS.
c      See Ref 1 for more complete instructions, Ref 2 for theory.
c    Combinations 0 5 7, 8 5 7, and 9 5 7 are recommended.  Others may
c    work well in a given design space.  Using the initial design, three
c    or four runs with different combinations should result in a most
c    improved design which can then be used as the initial design for
c    further optimization.  The three integers are:
c   ENTRY                                                  READ TO     DATA
c   ORDER          DESCRIPTION                            VARIABLE     TYPE
c   first    optimization strategy used by ADS            ISTRAT     integer
c             0 Go directly to the optimizer
c             6 Sequential Linear Programming
c             7 Method of Centers (Design must be feasible)
c             8 Sequential Quadratic Programming
c             9 Sequential Convex Programming
c  second    optimizer to be used by ADS                   IOPT      integer
c             4 Method of Feasible Directions
c             5 Modified Method of Feasible Directions
c   third    one dimensional search options                IONED     integer
c             5 Golden Section Method
c             6 Golden Section Method Plus Polynomial Interpolation
c             7 Bounded Polynomial Interpolation
c             8 Unbounded Polynomial Interpolation
c - - - - - - - - - - - - - - - - - - - - - - - - - - - - - - - - - - - - -
c    OUTPUT FILE: Named in TAPIN.DAT, consists of NTIME+1 rows of
c    three columns.  Format is list-directed from DP variables.
c     COLUMN                                              WRITTEN FROM
c     NUMBER           DESCRIPTION                          VARIABLE
c      one     times output from P-T GENERATOR            TIME(I), I=0,NTIME
c      two     P's from P-T GEN'R at each time           PRESS(I), I=0,NTIME
c      three   int. P's for each time from DPTGEN  PCOMPAR(I), I=0,NTIME
c - - - - - - - - - - - - - - - - - - - - - - - - - - - - - - - - - - - - -
c    SCREEN OUTPUT:  Outputs initial and final design values plut the
c     number of calls to the P-T History Generator.
c    INITIAL AND FINAL VALUES
c      DESCRIPTION                                         VARIABLE
c       lengths of tapered charge segments (ft)          TAP(I),I=1,NTAP
c       diameters of tapered charge        (in)          DIAM(I),I=0,NTAP
c       charge weight                      (lb)              WEIGHT
c       standoff                           (ft)              RANGE
c       sqrt of average sq diff of Pdesign-Pdesired           OBJ
c    OPTIMIZATION EFFICIENCY
c       number of calls to P-T generator                     NCALLS
c - - - - - - - - - - - - - - - - - - - - - - - - - - - - - - - - - - - - -
c VARIABLES
c    NAME     DATA   COMMON      ASSIGNED       USED     DESCRIPTION  ADS
c             TYPE                  BY           BY                    arg
c                                                                       ?
c A(I,J),      DP      -           ADS        ADS only    Constr grads  Y
c  I=1,NRA;,J=1,NCOLA
c DF(21)       DP      -           ADS        ADS only     Obj grads    Y
c DIAM(I),     DP    OPTDPA   TAPIN.DAT,MAIN    MAIN,    Charge diams   N
c  I=1,NTAP+1                                 PTGEN'R
c G(I),        DP      -           MAIN         ADS      Constraints    Y
c  I=1,NCON
c I             I      -           MAIN         MAIN    Local indexing  N
c IC(I),        I      -           ADS        ADS only   Gradient ID    Y
c  I=1,NCON
c IDG(I),       I      -           MAIN         ADS     Constraint ID   Y
c  I=1,NCON
```

```
c IGRAD        I      -          MAIN         ADS      Grad Calc Ctrl Y
c INFO         I      -        MAIN.ADS     MAIN.ADS   Prog Flow Ctrl Y
c IONED        I      -          user         ADS      One-D Search   Y
c IOPT         I      -          MAIN         ADS        Optimizer    Y
c IPRINT       I      -          MAIN         ADS      ADS Print Opts Y
c ISTRAT       I      -          user         ADS        Strategy     Y
c IWK(I),      I      -        ADS.MAIN       ADS       Work Array    Y
c  I=1,NRIWK
c NAMFIL      CH      -        TAPIN.DAT      MAIN      Output File   N
c NCALLS       I      -          MAIN         MAIN     PTGEN'R calls  N
c NCOLA        I      -          MAIN         ADS      No. A columns  Y
c NCON         I      -          MAIN         ADS     No. constraints Y
c NDES         I  FORDPTGEN  PROFIN.DAT      DPTGEN   Des'd plot sts-1 N
c NDV          I      -          MAIN         ADS     No. Design vars Y
c NGT          I      -          ADS          ADS       Gradient ctrl Y
c NRA          I      -          MAIN         ADS         A rows      Y
c NRIWK        I      -          MAIN         ADS      IWK Dimension  Y
c NRWK         I      -          MAIN         ADS       WK Dimension  Y
c NTAP         I     OPTI      TAPIN.DAT  PTGEN'R,MAIN  No. Chg Segs  N
c NTIME        I     OPTI       PTGEN'R  DPTGEN,DCOMPAR   Plt sts-1   N
c OBJ         DP      -          MAIN       MAIN ADS     Obj Func Val Y
c PCOMPAR(I). DP  FORDPTGEN     DPTGEN      DCOMPAR    Interp'd Press N
c  I=0,NDES
c PDES(I)     DP  FORDPTGEN    PROFIN.DAT    DPTGEN     Desired Press N
c  I=0,NDES
c PRESS(I)    DP    OPTDPA     PTGEN'R    PCOMPAR,MAIN    Calc Press  N
c  I=0,NTIME
c RANGE       DP    OPTDP    TAPIN.DAT,MAIN   PTGEN'R       Standoff   N
c SUMSQ       DP  FORDCOMPAR   DCOMPAR        MAIN       Press var'n  N
c TAP(I)      DP    OPTDPA   TAPIN.DAT,MAIN PTGEN'R,MAIN  Chg Seg Lth  N
c  I=1,NTAP
c TCO         DP    OPTDP      TAPIN.DAT    PTGEN'R     Surf CO Time  N
c TDES(I),    DP  FORDPTGEN    PROFIN.DAT   DPTGEN      Des'd PT Time N
c  I=0,NDES
c TIME(I)     DP    OPTDPA     PTGEN'R  DPTGEN,DCOMPAR,MAIN Calc time N
c  I=0,NTIME
c TLEN        DP    OPTDP      TAPIN.DAT     PTGEN'R    Lngth PT hist N
c VLB(I),     DP     -          MAIN          ADS        L lim on DV  Y
c  I=1,NDV
c VUB(I),     DP     -          MAIN          ADS        U lim on DV  Y
c  I=1,NDV
c WEIGHT      DP    PASS        DTAPWT        MAIN      Charge Weight N
c WK(I),      DP     -        ADS, MAIN       ADS        Work Array   Y
c  I=1,NRWK
c X(I),       DP     -        MAIN, ADS       ADS          Des Vas    Y
c  I=1,NDV
c - - - - - - - - - - - - - - - - - - - - - - - - - - - - - - - - - - - -
c SUBROUTINES
c  ADS(INFO,ISTRAT,IOPT,IONED,IPRINT,IGRAD,NDV,NCON,X,VLB,VUB,OBJ,
c            G,IDG,NGT,IC,DF,A,NRA,NCOLA,WK,NRWK,IWK,NRIWK)
c   See Ref 1 for more complete instructions. Ref 2 for theory.
c   Simply, ADS inputs design variables, constraints, and the objective
c    function for an initial design, then modifies that design,
c    requesting the corresponding objective and constraint values from
c    the calling program.
c   ARGUMENT VARIABLES
c    A(NRA,NCOLA) DP Array of constraint grads.  ADS use only here.
c    DF(NDV+1)    DP Array of objective gradients. ADS use only here.
c    G(NCON)      DP Array of constraints for current design in X
c     G(1&2): 25#<WEIGHT<125#: G(3-5): DIAM(1)<DIAM(2)<DIAM(3)<DIAM(4)
```

```
c     IC(NGT)        I  Array of constraint ID's.  NA this program
c     IDG(NCON)      I  Array ID'ing type of constraints: 0 for nonlin ineq
c     IGRAD          I  =0 for ADS calculate gradients using FD.
c     INFO           I  ADS flow control parameter.
c     IONED          I  =5,6,7,8:  See input section.
c     IOPT           I  =4,5: See input section.
c     IPRINT         I  =0000 FOR NO ADS PRINTOUT
c     ISTRAT         I  =0,6,7,8,9:  See input section
c     IWK(NRIWK)     I  Stores ADS I vars.  Some modifiable.
c     NCOLA          I  Dimensioned columns of A, min NDV+1.
c     NCON           I  Number of constraints in G.
c     NDV            I  Number of design variables in X.
c     NGT            I  Returned to by ADS for gradients.  0 this program.
c     NRA            I  Dimensioned A rows:  at least NDV+1.
c     NRIWK          I  Est: 200+NDV+NCON+N+MAX(N,2*NDV),N=MAX(NDV,NCOLA)
c     NRWK           I  Est: 500+10*(NDV+NCON)+NCOLA*(NCOLA+3)+N*(N/2)+1
c     OBJ           DP Objective function value. SUMSQ provided by DCOMPAR
c     VLB(NDV+1)    DP Array of design variable lower bounds. indices as X
c     VUB(NDV+1)    DP Array of design variable upper bounds. indices as X
c     WK            DP Array for ADS double precision variables.
c     X(NDV+1)      DP Array of design vars. Assigned by input, then ADS.
c      X(I)=TAP(I), I=1,3;       X(4+I)=DIAM(I), I=0,3       ; X(8)=RANGE
c      VLB(I)=1"                 VLB(4+I)=0.75"                VLB(8)=5'
c      VUB(I)=10'                VUB(4+I)=10"                  VUB(8)=30'
c   DCOMPAR
c    Communicates via COMMONS: OPTI, OPTDPA, FORDPTGEN, FORDCOMPAR
c    Input variables:  NTIME; PCOMPAR(I), PRESS(I), I=0,NTIME
c    Output variable:  SUMSQ
c   DPTGEN
c    Communicates via COMMONS: OPTI, OPTDPA, FORDPTGEN
c    Input variables:  NTIME; TIME(I), I=0,NTIME
c                      NDES;  TDES(I), PDES(I), I=0,NDES
c    Output variables: PCOMPAR(I), I=1,NTIME
c   DTAPWT
c    Communicates via COMMONS:  OPTI, OPTDPA, PASS
c    Input variables:   NTAP; DIAM(I),I=0,NTAP, TAP(I),I=1,NTAP
c    Output variables:  WIEGHT
c   PRESSURE-TIME HISTORY GENERATOR
c    Communicates via COMMONS:  OPTI, OPTDP, OPTDPA
c    Input variables:  NTAP; RANGE; TLEN; TCO; TAP(I), I=1,NTAP; DIAM(I),
c     I=0,NTAP.
c    Output variables:  NTIME; TIME(I), PRESS(I), I=0,NTIME
c   ****************************************************************
c
      PROGRAM DTAPOPT
      IMPLICIT NONE
C                                  SPECIFICATIONS FOR SUB VARIABLES
      COMMON/OPTI/NTAP,NTIME
      INTEGER     NTAP,NTIME
      COMMON/OPTDP/    RANGE,TLEN,TCO
      DOUBLE PRECISION RANGE,TLEN,TCO
      COMMON/OPTDPA/   TAP,    DIAM,      TIME,        PRESS
      DOUBLE PRECISION TAP(10),DIAM(0:10),TIME(0:1000),PRESS(0:1000)
      COMMON/PASS/     WEIGHT
      DOUBLE PRECISION WEIGHT
      COMMON/FORDPTGEN/NDES,TDES,        PDES,        PCOMPAR
      INTEGER          NDES
      DOUBLE PRECISION      TDES(0:1000),PDES(0:1000),PCOMPAR(0:1000)
      COMMON/FORDCOMPAR/SUMSQ
      DOUBLE PRECISION  SUMSQ
```

```
C                                       SPECIFICATIONS FOR ADS VARIABLES
C                                       up to 20 X's. 100 G's. 30 const grads
      INTEGER IWK(2000),IDG(100),IC(30)
      DOUBLE PRECISION X(21),VLB(21),VUB(21),G(100),DF(21), A(21,30),
     c WK(10000)
      INTEGER NRA,NCOLA,NRWK,NRIWK,IGRAD,NDV,NCON,ISTRAT,IPRINT,IOPT,
     c IONED, INFO, NGT
      DOUBLE PRECISION OBJ
C                                       SPECIFICATIONS FOR SUBROUTINES
      EXTERNAL SDTAPER
      EXTERNAL DTAPWT
      EXTERNAL DPTGEN
      EXTERNAL DCOMPAR
      EXTERNAL ADS
C                                       SPECIFICATIONS FOR LOCAL VARIABLES
      INTEGER I,NCALLS
      CHARACTER*12 NAMFIL
C                                       BEGIN EXECUTION
      NCALLS=0
C                                       ADS ARRAY DIMENSIONS
      NRA=21
      NCOLA=30
      NRWK=10000
      NRIWK=2000
C                                       ADS PARAMETERS
C                       (no user provided gradients, 5 constraints)
C                 (# design variables determined in initial design section)
      IGRAD=0
      NCON=5
C                                       INPUT INITIAL DESIGN, OUTPUT FILE,
C                                       BOUND ON DESIGN VARIABLES
      OPEN(88,FILE='TAPIN.DAT',STATUS='OLD')
      READ(88,*)NTAP
      NDV=2*(NTAP+1)
C                                       1" < length of segment < 20'
      DO 99 I=1,NTAP
        READ(88,*)TAP(I)
        X(I)=TAP(I)
        VLB(I)=1.0D0/12.0D0
        VUB(I)=20.0D0
   99 CONTINUE
C                                       0.75" < joint diameter < 10"
      DO 100 I=1,NTAP+1
        READ(88,*)DIAM(I-1)
        X(NTAP+I)=DIAM(I-1)
        VLB(NTAP+I)=0.75D0
        VUB(NTAP+I)=10.0D0
  100 CONTINUE
C                                       5' < standoff < 30'
      READ(88,*)RANGE
      X(2*NTAP+2)=RANGE
      VLB(2*NTAP+2)=15.0D0
      VUB(2*NTAP+2)=30.0D0
C                                       INPUT LENGTH OF TIME RECORD,TCO
      READ(88,*)TLEN
      READ(88,*)TCO
C                                       INPUT DESIRED PRESSURE PROFILE
      READ(88,1000)NAMFIL
      CLOSE(88)
      OPEN(89,FILE=NAMFIL)
```

```
 1000 FORMAT(A12)
      OPEN(88,FILE='PROFIN.DAT',STATUS='OLD')
      READ(88,*)NDES
      DO 101 I=0,NDES
        READ(88,*)TDES(I),PDES(I)
  101 CONTINUE
      CLOSE(88)
C                                   ID FIVE NONLINEAR CONSTRAINTS
      IDG(1)=0
      IDG(2)=0
      IDG(3)=0
      IDG(4)=0
      IDG(5)=0
C                                   INPUT
C        (no ADS print, interractive,optimizer and search options)
      IPRINT=0000
      PRINT*,' ENTER ISTRAT,IOPT,IONED:  '
      READ*,ISTRAT,IOPT,IONED
C                                   OPTIMIZE
C                     (0 no override, -2 default override)
      INFO=-2
   10 CALL ADS(INFO,ISTRAT,IOPT,IONED,IPRINT,IGRAD,NDV,NCON,X,VLB,
     C VUB,OBJ,G,IDG,NGT,IC,DF,A,NRA,NCOLA,WK,NRWK,IWK,NRIWK)
C                                   IFS TO CONTROL FLOW USING ADS INFO
      IF(INFO.EQ.1) THEN
C                                   EVALUATE OBJECTIVE AND CONSTRAINTS
C                                   ADS VARIABLES TO SDTAPER INPUT
        DO 102 I=1,NTAP
          TAP(I)=X(I)
  102   CONTINUE
        DO 103 I=1,NTAP+1
          DIAM(I-1)=X(NTAP+I)
  103   CONTINUE
        RANGE=X(2*NTAP+2)
C                                   CALCULATE PRESSURE PROFILE
        CALL SDTAPER
        NCALLS=NCALLS+1
C                                   CALCULATE WEIGHT
        CALL DTAPWT
C                                   CORRESPONDING DESIRED PRESSURES
        CALL DPTGEN
C                                   EVALUATE OBJECTIVE FUNCTION
        CALL DCOMPAR
        OBJ=SUMSQ
C                                   PRINT INITIAL DESIGN DATA TO SCREEN
        IF(NCALLS.EQ.1) THEN
          PRINT*,'      INITIAL DESIGN'
          PRINT1001,(TAP(I),I=1,NTAP)
          PRINT1002,(DIAM(I),I=0,NTAP)
          PRINT1003,WEIGHT
          PRINT1005,RANGE
          PRINT1004,OBJ
         ENDIF
C                                   EVALUATE CONSTRAINTS (25# < W < 125#)
        G(1)=(25.0D0-WEIGHT)
        G(2)=(WEIGHT-75.0D0)
C                                   EVALUATE CONSTRAINTS (D1<D2<D3<D4)
        G(3)=X(4)-X(5)
        G(4)=X(5)-X(6)
        G(5)=X(6)-X(7)
```

```
        GO TO 10
       ELSE
        IF(INFO.EQ.2) THEN
C                                   RESERVED FOR ADS GRADIENTS
          GO TO 10
        ELSE
          IF(INFO.EQ.-1) THEN
C                                   ADS OVERRIDE VALUES
c                 (for no scaling. rel FD step. min |FD step|.zero)

            IWK(2)=0
            WK(21)=0.001D0
            WK(22)=0.0001D0
            WK(26)=0.1D0
            WK(37)=1.0D-10
            GO TO 10
          ELSE
C                                   OPTIMIZATION COMPLETE. INFO=0

            IF(INFO.EQ.0) GO TO 20
          ENDIF
        ENDIF
      ENDIF
   20 CONTINUE
C                                   RECORD RESULTANT PRESSURE PROFILES
      DO 104 I=0,NTIME
        WRITE(89.*) TIME(I),PRESS(I),PCOMPAR(I)
  104 CONTINUE
      CLOSE(89)
C                                   PRINT DESIGN DATA TO SCREEN
      PRINT*
      PRINT*.'       FINAL DESIGN'
      PRINT1001.(TAP(I),I=1.NTAP)
 1001 FORMAT('          LENGTHS =     ',3F10.3,'          FT')
      PRINT1002,(DIAM(I),I=0.NTAP)
 1002 FORMAT('          DIAMETERS = '.4F10.2,' IN')
      PRINT1003,WEIGHT
 1003 FORMAT('          CHARGE WEIGHT =',F6.1,' LB')
      PRINT1005,RANGE
 1005 FORMAT('          RANGE =     ',F10.1,' FT')
      PRINT1004,OBJ
 1004 FORMAT('          SQRT OF AVG OF (Pdesign-Pdesired)^2 =', F6.1,
     c' PSI')
      PRINT*
      PRINT1006,NCALLS
 1006 FORMAT('        CALLS TO P-T HISTORY GENERATOR =',I4)
      END
```

II. SUBROUTINE DCOMPAR

```
c SUBROUTINE DCOMPAR
c    This subroutine, for use with DTAPOPT, computes the square root of
c  of the average sum of the squares of pressure differences.
c - - - - - - - - - - - - - - - - - - - - - - - - - - - - - - - - - - - - -
c  PRECISION:     DOUBLE
c  AUTHOR:        William Earl Miller II
c  LAST UPDATE:   6/17/92
c  INTERFACE:     4 BUSES:  OPTI, OPTDPA, FORDPTGEN, FORDCOMPAR.
```

```
c - - - - - - - - - - - - - - - - - - - - - - - - - - - - - - - - - - - -
c  VARIABLES
c    NAME                   TYPE   COMMON OR LOCAL   I/O?     DESCRIPTION
c   I                        I          local         na      local index
c   NTIME                    I          OPTI          I      calculated t
c   PCOMPAR(I.I=0.NTIME)    DP        FORDPTGEN       I    intp'd desired P
c   PRESS(I.I=0.NTIME)      DP         OPTDPA         I      calculated P
c   SUMSQ                   DP       FORDCOMPAR       0   value to be opt'd
c  ********************************************************************
      SUBROUTINE DCOMPAR
      IMPLICIT NONE
C                                  SPECIFICATIONS FOR GLOBAL VARIABLES
      COMMON/OPTI/NTAP,NTIME
      INTEGER      NTAP,NTIME
      COMMON/OPTDPA/   TAP.     DIAM.       TIME.          PRESS
      DOUBLE PRECISION TAP(10),DIAM(0:10).TIME(0:1000).PRESS(0:1000)
      COMMON/FORDPTGEN/NDES,TDES,          PDES.          PCOMPAR
      INTEGER          NDES
      DOUBLE PRECISION      TDES(0:1000).PDES(0:1000),PCOMPAR(0:1000)
      COMMON/FORDCOMPAR/SUMSQ
      DOUBLE PRECISION  SUMSQ
C                                  SPECIFICATIONS FOR LOCAL VARIABLE
      INTEGER I
C                                  BEGIN EXECUTION
      SUMSQ=0.0D0
      DO 99 I=0.NTIME
        SUMSQ=SUMSQ+(PCOMPAR(I)-PRESS(I))*(PCOMPAR(I)-PRESS(I))
   99 CONTINUE
      SUMSQ=SQRT(SUMSQ/(NTIME+1))
      RETURN
      END
```

III. SUBROUTINE DPTGEN

```
c  SUBROUTINE DPTGEN
c       This subroutine, for use with DTAPOPT. interpolates the input
c  desired pressure-time history to find the desired pressure at each
c  time computed by the P-T generator.
c - - - - - - - - - - - - - - - - - - - - - - - - - - - - - - - - - - - -
c  PRECISION:     DOUBLE
c  AUTHOR:        William Earl Miller II
c  LAST UPDATE:   6/17/92
c  INTERFACE:     3 BUSES:  OPTI, OPTDPA. FORDPTGEN
c - - - - - - - - - - - - - - - - - - - - - - - - - - - - - - - - - - - -
c  VARIABLES
c    NAME                   TYPE  COMMON OR LOCAL  I/O?     DESCRIPTION
c   I                        I         local        na     local index
c   J                        I         local        na     local index
c   NDES                     I       FORDPTGEN      I    No. input pts - 1
c   NTIME                    I         OPTI         I     No. calc pts - 1
c   PCOMPAR(I), I=0.NTIME   DP       FORDPTGEN      0    Int Desired Press
c   PDES(I). I=0,NDES       DP       FORDPTGEN      I     Input pressure
c   TDES(I), I=0,NDES       DP       FORDPTGEN      I       Input time
c   TIME(I), I=0.NTIME      DP        OPTDPA        I     Computed time
c *********************************************************************
      SUBROUTINE DPTGEN
      IMPLICIT NONE
C                                 SPECIFICATIONS FOR GLOBAL VARIABLES
      COMMON/OPTI/NTAP,NTIME
```

```
      INTEGER     NTAP,NTIME
      COMMON/OPTDPA/   TAP.    DIAM.      TIME.        PRESS
      DOUBLE PRECISION TAP(10),DIAM(0:10),TIME(0:1000),PRESS(0:1000)
      COMMON/FORDPTGEN/NDES,TDES,        PDES.        PCOMPAR
      INTEGER          NDES
      DOUBLE PRECISION      TDES(0:1000),PDES(0:1000),PCOMPAR(0:1000)
C                                SPECIFICATIONS FOR LOCAL VARIABLES
      INTEGER I,J
C                                BEGIN EXECUTION
      J=0
      IF((ABS(TIME(J)).GE.1.0D-13).AND.(ABS(TDES(J)).GE.1.0D-13)) THEN
        PRINT*,'INPUT PRESSURE PROFILE START TIME NOT ZERO'
        STOP
       ELSE
        TIME(J)=TDES(J)
      ENDIF
      DO 100 I=0,NTIME
    1   IF(TIME(I).GE.TDES(J)) THEN
          IF(TIME(I).LE.TDES(J+1)) THEN
            PCOMPAR(I)=PDES(J)+((TIME(I)-TDES(J))/(TDES(J+1)-TDES(J)))
     c                  *(PDES(J+1)-PDES(J))
            GO TO 100
          ENDIF
        ENDIF
        J=J+1
        IF(J.EQ.NDES+1) THEN
          PRINT*,'OUT OF INPUT PLOT POINTS'
          STOP
         ELSE
          GO TO 1
        ENDIF
  100 CONTINUE
      RETURN
      END
```

IV. SUBROUTINE DTAPWT

```
c     SUBROUTINE DTAPWT
c          This subroutine, for use with DTAPOPT, calculates the weight
c     of a tapered charge.
c - - - - - - - - - - - - - - - - - - - - - - - - - - - - - - - - - - - - -
c     PRECISION:     DOUBLE
c     AUTHOR:        William Earl Miller II
c     LAST UPDATE:   6/17/92
c     INTERFACE:     3 BUSES: OPTI, OPTDPA, PASS
c - - - - - - - - - - - - - - - - - - - - - - - - - - - - - - - - - - - - -
c     VARIABLES FROM COMMON STATEMENTS
c    NAME              TYPE    COMMON OR LOCAL  I/O?      DESCRIPTION
c     DIAM(I),I=0,NTAP DP        OPTDPA         I       Chg Diams (in)
c     I                I          local         na       local index
c     NTAP             I          OPTI          I        No. Chg Segs
c     PI               DP         local         na            Pi
c     RHO              DP         local         na    H20 dens (lbm/ft^3)
c     SGRAV            DP         local         na      Sp Grav of Chg
c     TAP(I),I=1,NTAP  DP        OPTDPA         I     Length of Seg (ft)
c     VOL              DP         local         na        Charge Vol
c     WEIGHT           DP         PASS          na      Charge Wt (lbm)
c  ******************************************************************
      SUBROUTINE DTAPWT
```

```
      IMPLICIT NONE
C                                       SPECIFICATIONS FOR GLOBAL VARIABLES
      COMMON/OPTI/NTAP,NTIME
      INTEGER     NTAP,NTIME
      COMMON/OPTDPA/   TAP,    DIAM,      TIME,        PRESS
      DOUBLE PRECISION TAP(10),DIAM(0:10),TIME(0:1000),PRESS(0:1000)
      COMMON/PASS/     WEIGHT
      DOUBLE PRECISION WEIGHT
C                                       SPECIFICATIONS FOR LOCAL VARIABLES
      DOUBLE PRECISION PI,RHO,SGRAV,VOL
      INTEGER I
C                                       BEGIN EXECUTION
      PI=4.0D0*ATAN(1.0D0)
      RHO= 62.32D0
      SGRAV= 1.712D0
      VOL=0.0D0
      DO 101 I=1,NTAP
      VOL=VOL+PI*TAP(I)*(DIAM(I-1)*DIAM(I-1)+DIAM(I)*DIAM(I)
     c +DIAM(I-1)*DIAM(I))/1728.0D0
  101 CONTINUE
      WEIGHT=VOL*SGRAV*RHO
      RETURN
      END
```

LIST OF REFERENCES

Belytschko, T. B., Lin, J. I., and Tsay, C. S., "Explicit Algorithms for Nonlinear Dynamics of Shells", *Computer Methods in Applied Mechanics and Engineering, Vol. 42*, pp. 225-251, 1984.

Bolt, B. A., *Nuclear Explosions and Earthquakes, The Parted Veil*, W. H. Freeman and Company, 1976.

Costanzo, F. A., "Tapered Charge Technology: Pressure History Calculation Using Program 'Taper' ", presentation at the Naval Postgraduate School, Monterey, California, 18 December, 1991.

Deruntz, J. A. Jr., "The Underwater Shock Analysis (USA) Code and Its Application", *The 60th Annual Shock and Vibration Symposium*, Vol. I, pp. 89-107, November, 1989.

Dobratz, B. M., *LLNL Explosives Handbook*, Lawrence Livermore National Laboratory, University of California, 1981.

Fox, P. K., *Nonlinear Dynamic Response of Cylindrical Shells Subjected to Underwater Side-On Explosions*, Master's Thesis, Naval Postgraduate School, March, 1992.

Fox, P. K., Kwon, Y. W., and Shin, Y. S., "Nonlinear Response of Cylindrical Shells to Underwater Explosion: Testing and Numberical Prediction Using USA/DYNA3D, Naval Postgraduate School Report NPS-ME-982-002, Monterey, California, March, 1992.

Glasstone, S., and Dolan, P. J., *The Effects Of Nuclear Weapons*, United States Department of Defense and the United States Department of Energy, 1977.

Gordon, J. T., and Davidson, D. K., "Calculation of the Shock Wave From a Pentolite Tapered Charge", *The Shock and Vibration Bulletin*, Vol. 53 Part 1, pp. 117-131, May, 1983.

Gurtman, G. A., Kirsch, J. W., and Hastings, C. R., "Analytical Equation of State for Water Compressed to 300 Kbar, *Journal of Applied Physics*, Vol. 42, No. 2, pp. 851-857, February, 1971.

Hallquist, J. O., and Stillman, D. W., *VEC/DYNA3D User's Manual (Nonlinear Dynamic Analysis of Structures in Three Dimensions)*, Livermore Software Technology Corporation Report 1018, June, 1990.

Hallquist, J. O., *LS-TAURUS: An Interactive Post-Processor For the Analysis Codes LS-NIKE3D, LS-DYNA3D, and TOPAZ3D (Command Documentation Manual)*, Livermore Software Technology Report 1001, April, 1990.

Lapp, E. L., "Atomic Bomb", *The World Book Encyclopedia*, Vol. 1, p. 843, 1980.

Meyers, M. S., and Murr, L. E., *Shock Waves and High Strain-Rate Phenomena in Metals; Concepts and Applications*, Plenum Press, 1981.

Shin, Y. S., and Geers, T. L., "Naval Ship Shock Design and Analysis", course notes, Naval Postgraduate School, Monterey, California, April, 1991.

Steinberg, D. J., "Spherical Explosions and the Equation of State of Water", Lawrence Livermore National Laboratory Report UCID-20974, p. 3, February, 1987.

Stillman, D. W., and Hallquist, J. O., *LS-INGRID: A Pre-Processor and Three-Dimensional Mesh Generator for the Programs LS-DYNA3D, LS-NIKE3D, and TOPAZ3D*, Livermore Software Technology Report 1019, June, 1991.

Ugural, A. C., and Fenster, S. K., Advanced Strength and Applied Elasticity, p. 398, Elsevier Science Publishing Co., 1987.

Vanderplaats, G. N., *Numerical Optimization Techniques for Engineering Design: With Applications*, McGraw-Hill Publishing Company, 1984.

Vanderplaats, G. N., *ADS - A FORTRAN Program For Automated Design Synthesis, Version 1.10*, program instructions, Naval Postgraduate School, Monterey, California, May, 1985.

INITIAL DISTRIBUTION LIST

1.	Defense Technical Information Center Cameron Station Alexandria, Virginia 22304-6145	2
2.	Library, Code 52 Naval Postgraduate School Monterey, California 93943-5002	2
3.	Professor Y. W. Kwon, Code ME/Kw Department of Mechanical Engineering Naval Postgraduate School Monterey, California 93943	1
4.	Professor Y. S. Shin, Code ME/Sg Department of Mechanical Engineering Naval Postgraduate School Monterey, California 93943	1
5.	Department Chairman, Code ME Department of Mechanical Engineering Naval Postgraduate School Monterey, California 93943	1
6.	Dr. Thomas T. Tsai Defense Nuclear Agency 6801 Telegraph Road Alexandria, Virginia 22310	1
7.	Dr. Kent Goering Defense Nuclear Agency 6801 Telegraph Road Alexandria, Virginia 22310	1
8.	Mr. Douglas Bruder Defense Nuclear Agency 6801 Telegraph Road Alexandria, Virginia 22310	1
9.	Naval Engineering Curricular Office (Code 34) Naval Postgraduate School Monterey, California 93943	1

10. Mr. Gene Remmers, ONT-23 1
Director, Office of Naval Technology
800 N. Quincy Street
Arlington, Virginia 22217-5000

11. Mr. Frederick A. Costanzo 1
David Taylor Research Center
Underwater Explosions Research Division
Code 177.1
Norfolk Naval Shipyard, Bldg. 369
Portsmouth, Virginia 23709-5000

12. Dr. Phillip B. Abraham 1
Office of Naval Research
Mechanics Division, Code 1132
800 North Quincy Street
Arlington, Virginia 22217-5000

13. LT William Earl Miller II 1
Long Beach Naval Shipyard
Code 338
Long Beach, California 90822